

Visualizing the Effects of Predictor Variables in Black Box Supervised Learning Models

Daniel W. Apley
Department of Industrial Engineering & Management Sciences
Northwestern University
Evanston, IL

Abstract: When fitting black box supervised learning models (e.g., complex trees, neural networks, boosted trees, random forests, nearest neighbors, local kernel-weighted methods, etc.), visualizing the main effects of the individual predictor variables and their low-order interaction effects is often important, and partial dependence (PD) plots are the most popular approach for accomplishing this. However, PD plots involve a serious pitfall if the predictor variables are far from independent, which is quite common with large observational data sets. Namely, PD plots require extrapolation of the response at predictor values that are far outside the multivariate envelope of the training data, which can render the PD plots unreliable. Although marginal plots (M plots) do not require such extrapolation, they produce substantially biased and misleading results when the predictors are dependent, analogous to the omitted variable bias in regression. We present a new visualization approach that we term accumulated local effects (ALE) plots, which inherits the desirable characteristics of PD and M plots, without inheriting their preceding shortcomings. Like M plots, ALE plots do not require extrapolation; and like PD plots, they are not biased by the omitted variable phenomenon. Moreover, ALE plots are far less computationally expensive than PD plots.

Keywords: Partial dependence plots; marginal plots; supervised learning; visualization; functional ANOVA

1. Introduction

Suppose we have fit a supervised learning model for approximating $E[Y|\mathbf{X} = \mathbf{x}] \cong f(\mathbf{x})$, where Y is a scalar response variable, $\mathbf{X} = (X_1, X_2, \dots, X_d)$ is a vector of d predictor variables (aka predictors), and $f(\cdot)$ is the fitted model that predicts Y as a function of \mathbf{X} . To simplify notation, we omit any $\hat{\cdot}$ symbol over f , with the understanding that it is fitted from data. The training data to which the model is fit consists of n $(d+1)$ -variate observations $\{y_i, \mathbf{x}_i = (x_{i,1}, x_{i,2}, \dots, x_{i,d}) : i = 1, 2, \dots, n\}$. Throughout, we use upper case to denote a random variable and lower case to denote specific or observed values of the random variable.

Our objective is to visualize and understand the "main effects" dependence of $f(\mathbf{x}) = f(x_1, x_2, \dots, x_d)$ on each of the individual predictors, and well as the low-order "interaction effects" among pairs of predictors, if present. The most popular approach for visualizing the effects of the predictors is partial dependence (PD) plots, introduced by Friedman (2001). For ease of exposition, throughout the introduction we illustrate concepts for the $d = 2$ case, but the general d case is treated in the remainder of the paper. To understand the effect of one predictor (say x_1) on the predicted response, a PD plot is a plot of the function

$$f_{1,PD}(x_1) \equiv E[f(x_1, X_2)] = \int p_2(x_2) f(x_1, x_2) dx_2 \quad (1)$$

versus x_1 , where $p_2(\cdot)$ denotes the marginal distribution of X_2 . Throughout, we use $p(\cdot)$, $p_{\cdot|}(\cdot | \cdot)$, and $p_{\cdot,}(\cdot, \cdot)$ to respectively denote the marginal, conditional, and joint probability density functions of various elements of \mathbf{X} , with the subscripts indicating which elements. An estimate of (1), calculated pointwise in x_1 for a range of x_1 values, is

$$\hat{f}_{1,PD}(x_1) \equiv \frac{1}{n} \sum_{i=1}^n f(x_1, x_{i,2}). \quad (2)$$

Figure 1(a) illustrates how $f_{1,PD}(x_1)$ is computed at a specific value $x_1 = 0.3$ for a toy example with $n = 200$ observations of (X_1, X_2) following a uniform distribution along the line segment $x_2 = x_1$ but with independent $N(0, 0.05^2)$ variables added to both predictors (see Hooker, 2007, for a similar example demonstrating the adverse consequences of extrapolation in PD plots). We return to this example in Section 4, where we generate response observations and

fit regression tree and neural network models $f(\mathbf{x})$ to the data, but for now we can ignore the response. The level of multicollinearity in (X_1, X_2) in Figure 1 is large enough that the integrand in (1) must be evaluated in regions that contain no data, but not so large that the effects of x_1 and x_2 cannot be distinguished.

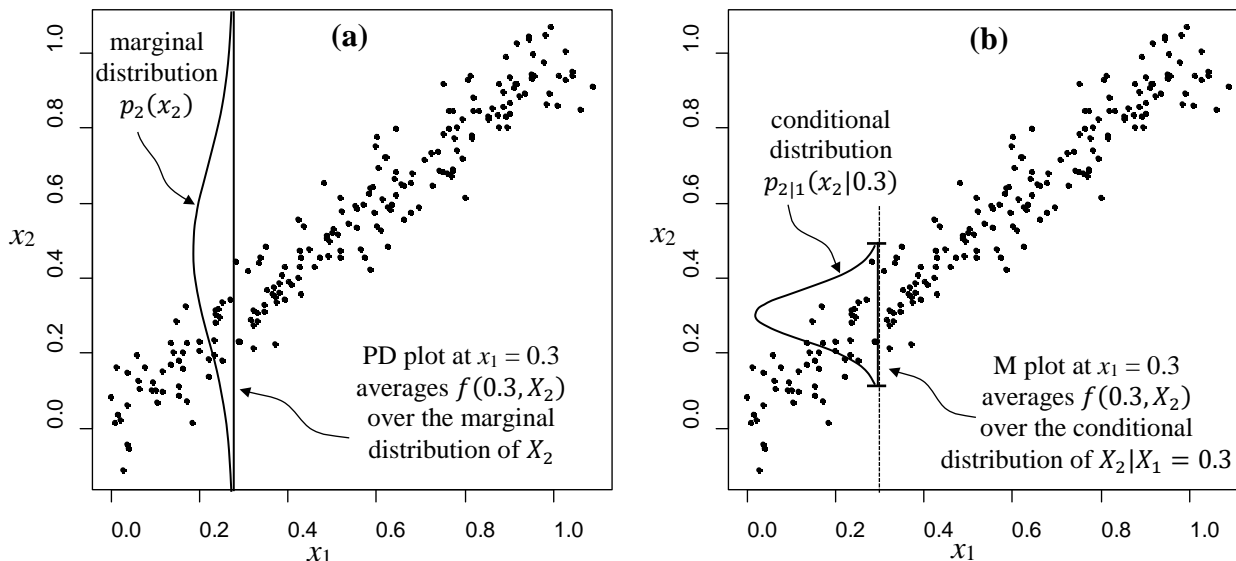


Figure 1. Illustration of the differences between the computation of (a) $f_{1,PD}(x_1)$ and (b) $f_{1,M}(x_1)$ at $x_1 = 0.3$.

The salient point in Figure 1(a), which illustrates the problem with PD plots, is that the integral in (1) is the weighted average of $f(x_1, X_2)$ as X_2 varies over its marginal distribution. This integral is over the entire vertical line segment in Figure 1(a) and requires rather severe extrapolation beyond the envelope of the training data. If one were to fit a simple parametric model of the correct form (e.g., $f(\mathbf{x}) = \beta_0 + \beta_1 x_1 + \beta_2 x_2^2$), then this extrapolation might be reliable. However, by nature of its flexibility, a nonparametric supervised learning model like a regression tree cannot be expected to extrapolate reliably. As we demonstrate in a continuation of this example in Section 4 (see Figures 5—7, later), this renders the PD plot an unreliable indicator of the effect of x_1 .

The extrapolation in Figure 1(a) that is required to calculate $f_{1,PD}(x)$ occurs because the marginal density $p_2(x_2)$ is much less concentrated around the data than the conditional density $p_{2|1}(x_2|x)$, due to the strong dependence between X_2 and X_1 . Marginal plots (M plots) are

alternatives to PD plots that avoid such extrapolation by using the conditional density in place of the marginal density. As illustrated in Figure 1(b), an M plot of the effect of x_1 is a plot of the function

$$f_{1,M}(x_1) \equiv E[f(X_1, X_2)|X_1 = x_1] = \int p_{2|1}(x_2|x_1)f(x_1, x_2)dx_2 \quad (3)$$

versus x_1 . A crude estimate of $f_{1,M}(x_1)$ is

$$\hat{f}_{1,M}(x_1) \equiv \frac{1}{n(x_1)} \sum_{i \in N(x_1)} f(x_1, x_{i,2}), \quad (4)$$

where $N(x_1) \subset \{1, 2, \dots, n\}$ is the subset of row indices i for which $x_{i,1}$ falls into some small, appropriately selected neighborhood of x_1 , and $n(x_1)$ is the number of observations in the neighborhood. Although more sophisticated kernel smoothing methods are typically used to estimate $f_{1,M}(x_1)$, we do not consider them here, because there is a more serious problem with using $f_{1,M}(x_1)$ to visualize the main effect of x_1 when X_1 and X_2 are dependent. Namely, using $f_{1,M}(x_1)$ is like regressing Y onto X_1 while ignoring (i.e., marginalizing¹ over) the nuisance variable X_2 . Consequently, if Y depends on X_1 and X_2 , $f_{1,M}(x_1)$ will reflect both of their effects, a consequence of the omitted variable bias phenomenon in regression.

The main objective of this paper is to introduce a new method of assessing the main and interaction effects of the predictors in black box supervised learning models that avoids the foregoing problems with PD plots and M plots. We refer to the approach as accumulated local effects (ALE) plots. For the case that $d = 2$ and $f(\cdot)$ is differentiable (the more general definition is deferred until Section 2), we define the ALE main-effect of x_1 as

$$\begin{aligned} f_{1,ALE}(x_1) &\equiv \int_{z_{0,1}}^{x_1} E[f^1(X_1, X_2)|X_1 = z_1]dz_1 - \text{constant} \\ &= \int_{z_{0,1}}^{x_1} \int p_{2|1}(x_2|z_1)f^1(z_1, x_2)dx_2 dz_1 - \text{constant}, \end{aligned} \quad (5)$$

¹ Regarding the terminology, plots of an estimate of $f_{1,M}(x_1)$ are often referred to as "marginal plots", because ignoring X_2 in this manner is equivalent to working with the joint distribution of (Y, X_1) after marginalizing across X_2 . Unfortunately, plots of $\hat{f}_{1,PD}(x_1)$ are also sometimes referred to as "marginal plots" (e.g., in the **gbm** package for fitting boosted trees in R), presumably because the integral in (1) is with respect to the marginal distribution $p_2(x_2)$. In this paper, marginal plots will refer to how we have defined them above.

where $f^1(x_1, x_2) \equiv \partial f(x_1, x_2) / \partial x_1$ represents the *local effect* of x_1 on $f(\cdot)$ at (x_1, x_2) , and $z_{0,1}$ is some value chosen near the lower bound of the effective support of $p_1(\cdot)$, e.g., just below the smallest observation $\min\{x_{i,1}: i = 1, 2, \dots, n\}$. Choice of $z_{0,1}$ is not important, as it only effects the vertical translation of the ALE plot of $f_{1,ALE}(x_1)$ versus x_1 , and the constant in (5) will be chosen to vertically center the plot (see Section 2 for details).

The function $f_{1,ALE}(x_1)$ can be interpreted as the *accumulated local effects* of x_1 in the following sense. In (5), we calculate the local effect $f^1(z_1, x_2)$ of x_1 at $(x_1 = z_1, x_2)$, then average this local effect across all values of x_2 with weight $p_{2|1}(x_2|z_1)$, and then finally accumulate/integrate this averaged local effect over all values of z_1 up to x_1 . As illustrated in Figure 2, when averaging the local effect $f^1(z_1, x_2)$ across x_2 , the use of the conditional density $p_{2|1}(x_2|z_1)$, instead of the marginal density $p_2(x_2)$, avoids the extrapolation required in PD plots. The avoidance of extrapolation is similar to M plots, which also use the conditional density $p_{2|1}(x_2|z_1)$. However, by averaging (across x_2) and accumulating (up to x_1) the local effects via (5), as opposed to directly averaging $f(\cdot)$ via (3), ALE plots avoid the omitted nuisance variable bias that renders M plots of little use for assessing the main effects of the predictors. This is closely related to the use of paired differences to block out nuisance factors in more general statistical settings, which we discuss in Section 5.1

It should be mentioned that there exist methods for visualizing the effects of predictors that plot a collection of curves, rather than a single curve that represents some aggregate effect. Consider the effect of a single predictor X_j , and let $\mathbf{X}_{\setminus j}$ denote the other predictors. Conditioning plots (coplots) (Chambers, 1992; Cleveland, 1993), conditional response (CORE) plots (Cook, 1995), and individual conditional expectation (ICE) plots (Goldstein, et al., 2014) plot quantities like $f(x_j, \mathbf{x}_{\setminus j})$ vs. x_j for a collection of discrete values of $\mathbf{x}_{\setminus j}$ (CORE and ICE plots), or similarly they plot $E[f(x_j, \mathbf{X}_{\setminus j}) | \mathbf{X}_{\setminus j} \in S_k]$ vs. x_j for each set S_k in some partition $\{S_k: k = 1, 2, \dots\}$ of the space of $\mathbf{X}_{\setminus j}$. Such a collection of curves have more in common with interaction effect plots (as in Figure 9, later) than with main effect plots, for which one desires, by definition, a single aggregated curve.

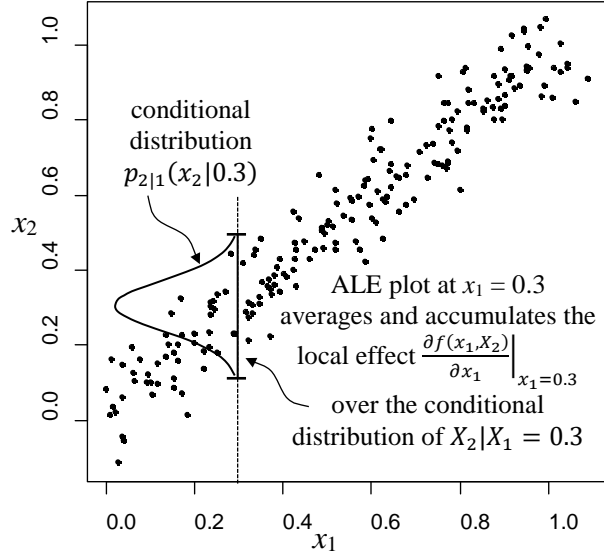


Figure 2. Illustration of the computation of $f_{1,ALE}(x_1)$ at $x_1 = 0.3$.

The format of the remainder of the paper is as follows. In Section 2, we define the ALE main effects for individual predictors and the ALE second-order interaction effects for pairs of predictors. In Section 3 we present an algorithm for estimating the ALE main and second-order interaction effects that involves finite difference versions of the differentiation and integration in (5). The paper focuses on main and second-order interaction effects, whereas general higher-order effects and their estimation are treated in the Appendices. The ALE plot estimation algorithm is conceptually straightforward and computationally efficient (much more efficient than PD plots) and does not require differentiability of $f(\mathbf{x})$. In Section 4 we give examples that illustrate the ALE plots and, in particular, how they can produce correct results when PD plots are badly biased due to their reliance on extrapolation. In Section 5, we discuss issues including various unbiasedness properties of ALE effects and their computational advantages, and we illustrate with a real data example. We also discuss their relation to functional ANOVA decompositions for dependent variables (e.g., Hooker, 2007) that have been developed to avoid the same extrapolation problem highlighted in Figure 1(a). ALE plots are far more computationally efficient and systematic to compute than functional ANOVA decompositions; and they yield a fundamentally different decomposition of $f(\mathbf{x})$ that is better suited for visualization of the effects of the

predictors. Section 6 concludes the paper. We also provide as supplementary material an R package **ALEPlot** to implement ALE plots.

2. Definition of ALE Main and Second-Order Effects

In this section we define the ALE main effects for each predictor (Eq. (5) is a special case for the first predictor x_1) and the ALE second-order effects for each pair of predictors. ALE plots are plots of estimates of these quantities, and the estimators are defined in Section 3. We do not envision ALE plots being commonly used to visualize third-and-high-order effects, since high-order effects are difficult to interpret and usually not as predominant as main and second-order effects. For this reason, and to simplify notation, we focus on main and second-order effects, and we relegate the definition of higher-order ALE effects to the appendices. Mainly for notational simplicity, we define the ALE effects for the case of differentiable $f(\cdot)$. The sample estimators defined in Section 3 apply directly to either differentiable or nondifferentiable $f(\cdot)$, and we discuss in Remark 2 below how to extend the definition of the theoretical ALE effects to nondifferentiable $f(\cdot)$.

For each $j \in \{1, 2, \dots, d\}$, let $\mathbf{X}_{\setminus j}$ denote the subset of $d - 1$ predictors excluding X_j , i.e., $\mathbf{X}_{\setminus j} = (X_k: k = 1, 2, \dots, d; k \neq j)$, and let $f^j(x_j, \mathbf{x}_{\setminus j}) \equiv \partial f(x_j, \mathbf{x}_{\setminus j}) / \partial x_j$ denote the partial derivative of $f(\mathbf{x})$ with respect to x_j . Let $\mathbf{z}_0 = (z_{0,1}, z_{0,2}, \dots, z_{0,d})$ be approximate lower bounds for each element of (X_1, X_2, \dots, X_d) , analogous to $z_{0,1}$ in (5).

The uncentered ALE main (aka first-order) effect of x_j is defined as

$$\begin{aligned} \tilde{f}_{j,ALE}(x_j) &\equiv \int_{z_{0,j}}^{x_j} E[f^j(X_j, \mathbf{X}_{\setminus j}) | X_j = z_j] dz_j \\ &= \int_{z_{0,j}}^{x_j} \int p_{\setminus j|j}(\mathbf{x}_{\setminus j} | z_j) f^j(z_j, \mathbf{x}_{\setminus j}) d\mathbf{x}_{\setminus j} dz_j. \end{aligned} \quad (6)$$

The ALE main effect of x_j , denoted by $f_{j,ALE}(x_j)$, is defined the same as $\tilde{f}_{j,ALE}(x_j)$ but centered so that $f_{j,ALE}(X_j)$ has a mean of zero with respect to the marginal distribution of X_j . That is,

$$\begin{aligned} f_{j,ALE}(x_j) &\equiv \tilde{f}_{j,ALE}(x_j) - E[\tilde{f}_{j,ALE}(X_j)] \\ &= \tilde{f}_{j,ALE}(x_j) - \int p_j(z_j) \tilde{f}_{j,ALE}(z_j) dz_j, \end{aligned} \quad (7)$$

To define the ALE second-order effects, for each pair of indices $\{j, l\} \subseteq \{1, 2, \dots, d\}$, let $\mathbf{X}_{\setminus\{j,l\}}$ denote the subset of $d - 2$ predictors excluding $\{X_j, X_l\}$, i.e., $\mathbf{X}_{\setminus\{j,l\}} = (X_k: k = 1, 2, \dots, d; k \neq j; k \neq l)$. Let $f^{\{j,l\}}(x_j, x_l, \mathbf{x}_{\setminus\{j,l\}}) \equiv \partial^2 f(x_j, x_l, \mathbf{x}_{\setminus\{j,l\}}) / \partial x_j \partial x_l$ denote the second-order partial derivative of $f(\mathbf{x})$ with respect to x_j and x_l . The uncentered ALE second-order effect of $\{x_j, x_l\}$ is defined as

$$\begin{aligned} \tilde{f}_{\{j,l\},ALE}(x_j, x_l) &\equiv \int_{z_{0,l}}^{x_l} \int_{z_{0,j}}^{x_j} E[f^{\{j,l\}}(X_j, X_l, \mathbf{X}_{\setminus\{j,l\}}) | X_j = z_j, X_l = z_l] dz_j dz_l \\ &= \int_{z_{0,l}}^{x_l} \int_{z_{0,j}}^{x_j} \int p_{\setminus\{j,l\}|\{j,l\}}(\mathbf{x}_{\setminus\{j,l\}} | z_j, z_l) f^{\{j,l\}}(z_j, z_l, \mathbf{x}_{\setminus\{j,l\}}) d\mathbf{x}_{\setminus\{j,l\}} dz_j dz_l. \end{aligned} \quad (8)$$

The ALE second-order effect of $\{x_j, x_l\}$, denoted by $f_{\{j,l\},ALE}(x_j, x_l)$, is defined the same as $\tilde{f}_{\{j,l\},ALE}(x_j, x_l)$ but "doubly centered" so that $f_{\{j,l\},ALE}(X_j, X_l)$ has a mean of zero with respect to the marginal distribution of $\{X_j, X_l\}$ and so that the ALE main effects of x_j and x_l on $f_{\{j,l\},ALE}(X_j, X_l)$ are both zero. The latter centering is accomplished by subtracting from $\tilde{f}_{\{j,l\},ALE}(x_j, x_l)$ its uncentered ALE main effects via

$$\begin{aligned} \tilde{f}_{\{j,l\},ALE}(x_j, x_l) &\equiv \tilde{f}_{\{j,l\},ALE}(x_j, x_l) - \int_{z_{0,j}}^{x_j} E \left[\partial \tilde{f}_{\{j,l\},ALE}(X_j, X_l) / \partial X_j | X_j = z_j \right] dz_j - \\ &\quad - \int_{z_{0,l}}^{x_l} E \left[\partial \tilde{f}_{\{j,l\},ALE}(X_j, X_l) / \partial X_l | X_l = z_l \right] dz_l \\ &= \tilde{f}_{\{j,l\},ALE}(x_j, x_l) - \int_{z_{0,j}}^{x_j} \int p_{l|j}(z_l | z_j) \partial \tilde{f}_{\{j,l\},ALE}(z_j, z_l) / \partial z_j dz_l dz_j - \\ &\quad - \int_{z_{0,l}}^{x_l} \int p_{j|l}(z_j | z_l) \partial \tilde{f}_{\{j,l\},ALE}(z_j, z_l) / \partial z_l dz_j dz_l. \end{aligned} \quad (9)$$

The former centering is accomplished by taking

$$\begin{aligned} f_{\{j,l\},ALE}(x_j, x_l) &\equiv \tilde{f}_{\{j,l\},ALE}(x_j, x_l) - E[\tilde{f}_{\{j,l\},ALE}(X_j, X_l)] \\ &= \tilde{f}_{\{j,l\},ALE}(x_j, x_l) - \int \int p_{\{j,l\}}(z_j, z_l) \tilde{f}_{\{j,l\},ALE}(z_j, z_l) dz_j dz_l. \end{aligned} \quad (10)$$

It can be verified that $f_{\{j,l\},ALE}(x_j, x_l)$ is centered in the sense that the ALE main effects of x_j and x_l on $f_{\{j,l\},ALE}(x_j, x_l)$ are both zero (see Appendix B for a formal proof of a related but more general result).

If we define the zero-order effect for any function of \mathbf{X} as its expected value with respect to the distribution of \mathbf{X} , then we can view the ALE first-order effect of x_j as being obtained by first

calculating its uncentered first-order effect (6), and then for the resulting function, calculating and subtracting its zero-order effect. Likewise, the ALE second-order effect of $\{x_j, x_l\}$ is obtained by first calculating the uncentered second-order effect (8), then for the resulting function, calculating and subtracting both of its first-order effects of x_j and of x_l , and then for this resulting function, calculating and subtracting its zero-order effect. The ALE higher-order effects are defined analogously in Appendix A. The uncentered higher-order effect is first calculated, and then all lower-order effects are sequentially calculated and subtracted one order at a time, until the final result has all lower-order effects that are identically zero.

Remark 1: In Appendix B we show that a function $f(\mathbf{x})$ can be decomposed into $f(\mathbf{x}) = \sum_{j=1}^d f_{j,ALE}(x_j) + \sum_{j=1}^d \sum_{l=j+1}^d f_{\{j,l\},ALE}(x_j, x_l) + \sum_{J \subseteq \{1,2,\dots,d\}, |J| \geq 3} f_{J,ALE}(\mathbf{x}_J)$, where the third summation is over the ALE third- and-higher-order interaction effects, as defined in Appendix A, and $|J|$ denotes the cardinality of a set of predictor indices J . We also show in Appendix B that the ALE decomposition has the following orthogonality-like property. Let $J \subseteq \{1, 2, \dots, d\}$ and $J' \subseteq \{1, 2, \dots, d\}$ be any two subsets of predictor indices (possibly having some predictors in common). The ALE $|J|$ -order effect of the predictors \mathbf{X}_J for the function $f_{J',ALE}$ is identically zero when $J \neq J'$; and the ALE $|J|$ -order effect of the predictors \mathbf{X}_J for the function $f_{J,ALE}$ is the same function $f_{J,ALE}$. For example, consider any pair of predictors $\{x_j, x_l\}$. The ALE main effect of any predictor (including x_j or x_l) for the function $f_{\{j,l\},ALE}(x_j, x_l)$ is identically zero. Thus all ALE second-order interaction effect functions have ALE main effects that are all identically zero. Likewise, all ALE main effect functions have ALE second-order interaction effects that are all identically zero. And for the function $f_{\{j,l\},ALE}(x_j, x_l)$, the ALE second-order interaction effect of any other pair of predictors is identically zero. Similarly, the ALE first- and second-order interaction effects for any ALE third-order effect function are all identically zero, and vice-versa. The ALE decomposition is reminiscent of functional ANOVA decompositions, which we discuss in Section 5.3.

Remark 2: Definition of $f_{j,ALE}(x_j)$ and $f_{\{j,l\},ALE}(x_j, x_l)$ for nondifferentiable $f(\cdot)$. The preceding definitions of the ALE effects assume differentiability of $f(\cdot)$. For nondifferentiable $f(\cdot)$ (e.g., tree-based models, to which we certainly want the visualization approach to be

applicable), we can replace the first-order derivatives $f^J(x_j, \mathbf{x}_{\setminus j})$ and the second-order derivatives $f^{\{j,l\}}(x_j, x_l, \mathbf{x}_{\setminus \{j,l\}})$ by corresponding finite differences and then replace the integrals in the first lines of (6) and (8) by finite summations over the same increments used in the finite differences. Taking the limit as the increments approach zero would extend the definitions of ALE first-order and second-order effects for nondifferentiable $f(\cdot)$. However, we do not further develop the definition here, because the estimators $\hat{f}_{j,ALE}(x_j)$ and $\hat{f}_{\{j,l\},ALE}(x_j, x_l)$ defined in Section 3 are always calculated via finite differences, regardless of whether $f(\cdot)$ is differentiable. Our intention is that the ALE effect functions are estimated for a model $f(\cdot)$ using the same sample of training data that was used to fit $f(\cdot)$, as opposed to calculated via (6)—(10) using some expression for the distribution $p_{\{1,2,\dots,d\}}(\mathbf{x})$ of \mathbf{X} .

3. Estimation of $f_{j,ALE}(x_j)$ and $f_{\{j,l\},ALE}(x_j, x_l)$

Estimation of the ALE first-order and second-order effects is the primary objective in this paper. We view ALE plots as a tool to visualize the low-order effects of the predictors on a supervised learning model $f(\cdot)$ fitted to a sample of training data. In Appendix C we describe how to estimate the ALE higher-order effect $f_{J,ALE}(\mathbf{x}_J)$ for a general subset $J \subseteq \{1, 2, \dots, d\}$ of predictor indices, which is conceptually the same as, but requires more tedious notation than the special cases of first-order ($|J| = 1$) and second-order ($|J| = 2$) effects that we treat in this section. The estimate $\hat{f}_{J,ALE}$ is obtained by computing estimates of the quantities in Eqs. (6)—(10) for $J = j$ (a single index) and $J = \{j, l\}$ (a pair of indices). The estimate of each quantity is obtained by (i) replacing the derivative $f^J(\mathbf{X}_J, \mathbf{X}_{\setminus J})$ by the corresponding finite difference for some appropriate discretization of the \mathbf{X}_J predictor space; (ii) replacing the expectation $E[f^J(\mathbf{X}_J, \mathbf{X}_{\setminus J}) | \mathbf{X}_J = \mathbf{z}_J]$ by its corresponding sample average across all $\mathbf{x}_{i,\setminus J}$ ($i = 1, 2, \dots, n$) for which $\mathbf{x}_{i,J}$ falls into the same discrete cell as \mathbf{z}_J ; and (iii) replacing the outer integral by the corresponding summation over the same discretization used when calculating the finite differences. In the preceding, $\mathbf{x}_{i,J} = (x_{i,j}: j \in J)$ and $\mathbf{x}_{i,\setminus J} = (x_{i,j}: j = 1, 2, \dots, d; j \notin J)$ denote the i th observation of the subsets of predictors \mathbf{X}_J and $\mathbf{X}_{\setminus J}$, respectively.

More concretely, for each $j \in \{1, 2, \dots, d\}$, let $\{N_j(k) = (z_{k-1,j}, z_{k,j}]: k = 1, 2, \dots, K\}$ be a sufficiently fine partition of the sample range of $\{x_{i,j}: i = 1, 2, \dots, n\}$ into K intervals. In all of our examples later in the paper, we chose $z_{k,j}$ as the k/K quantile of the empirical distribution of $\{x_{i,j}: i = 1, 2, \dots, n\}$ with $z_{0,j}$ chosen just below the smallest observation, and $z_{K,j}$ chosen as the largest observation. Figure 3 illustrates the notation and concepts in computing the ALE main effect estimator $\hat{f}_{j,ALE}(x_j)$ for the first predictor $j = 1$ for the case of $d = 2$ predictors. For $k = 1, 2, \dots, K$, let $n_j(k)$ denote the number of training observations that fall into the k th interval $N_j(k)$, so that $\sum_{k=1}^K n_j(k) = n$. For a particular value x of the predictor x_j , let $k_j(x)$ denote the index of the interval into which x falls, i.e., $x \in (z_{k_j(x)-1,j}, z_{k_j(x),j}]$.

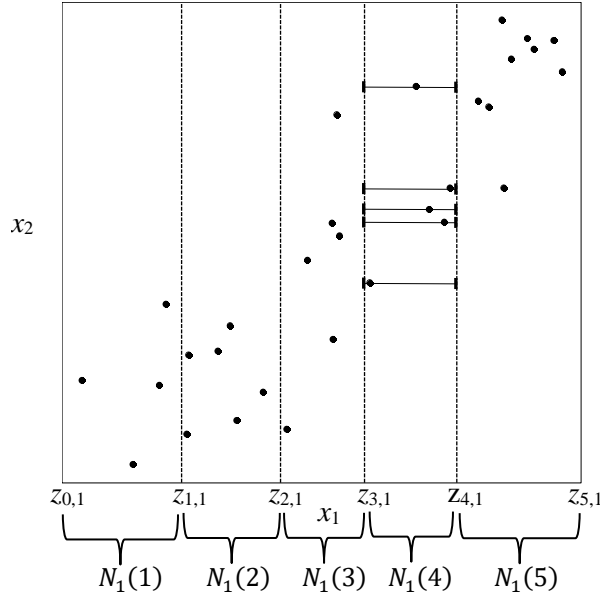


Figure 3. Illustration of the notation and concepts in computing the ALE main effect estimator $\hat{f}_{j,ALE}(x_j)$ for $j = 1$ with $d = 2$ predictors. The bullets are a scatterplot of $\{(x_{i,1}, x_{i,2}): i = 1, 2, \dots, n\}$ for $n = 30$ training observations. The range of $\{x_{i,1}: i = 1, 2, \dots, n\}$ is partitioned into $K = 5$ intervals $\{N_1(k) = (z_{k-1,1}, z_{k,1}]: k = 1, 2, \dots, 5\}$ (in practice, K should usually be chosen much larger than 5). The numbers of training observations falling into the 5 intervals are $n_1(1) = 4$, $n_1(2) = 6$, $n_1(3) = 6$, $n_1(4) = 5$, and $n_1(5) = 9$. The horizontal line segments shown in the $N_1(4)$ region are the segments across which the finite differences $f(z_{4,j}, \mathbf{x}_{i,\setminus j}) - f(z_{3,j}, \mathbf{x}_{i,\setminus j})$ are calculated and then averaged in the inner summand of Eq. (11) corresponding to $k = 4$ and $j = 1$.

For general d , to estimate the main effect function $f_{j,ALE}(\cdot)$ of a predictor x_j , we first compute an estimate of the uncentered effect $\tilde{f}_{j,ALE}(\cdot)$ defined in (6), which is

$$\hat{\tilde{f}}_{j,ALE}(x) = \sum_{k=1}^{k_j(x)} \frac{1}{n_j(k)} \sum_{\{i: x_{i,j} \in N_j(k)\}} [f(z_{k,j}, \mathbf{x}_{i,\setminus j}) - f(z_{k-1,j}, \mathbf{x}_{i,\setminus j})] \quad (11)$$

for each $x \in (z_{0,j}, z_{K,j}]$. Paralleling (7), the ALE main effect estimate of $f_{j,ALE}(\cdot)$ is then obtained by subtracting an estimate of $E[\tilde{f}_{j,ALE}(X_j)]$ from (11), i.e.,

$$\begin{aligned} \hat{f}_{j,ALE}(x) &= \hat{\tilde{f}}_{j,ALE}(x) - \frac{1}{n} \sum_{i=1}^n \hat{\tilde{f}}_{j,ALE}(x_{i,j}) \\ &= \hat{\tilde{f}}_{j,ALE}(x) - \frac{1}{n} \sum_{k=1}^K n_j(k) \hat{\tilde{f}}_{j,ALE}(z_{k,j}). \end{aligned} \quad (12)$$

To estimate the ALE second-order effect of a pair of predictors $\{x_j, x_l\}$, we partition the $\{x_j, x_l\}$ space into a grid of K^2 rectangular cells obtained as the cross product of the individual one-dimensional partitions. Figure 4 illustrates the notation and concepts. Let (k, m) (with k and m integers between 1 and K) denote the indices into the grid of rectangular cells with k corresponding to x_j and m corresponding to x_l . In analogy with $N_j(k)$ and $n_j(k)$ defined in the context of estimating $f_{j,ALE}(\cdot)$, let $N_{\{j,l\}}(k, m) = N_j(k) \times N_l(m) = (z_{k-1,j}, z_{k,j}] \times (z_{m-1,l}, z_{m,l}]$ denote the cell associated with indices (k, m) , and let $n_{\{j,l\}}(k, m)$ denote the number of training observations that fall into cell $N_{\{j,l\}}(k, m)$, so that $\sum_{k=1}^K \sum_{m=1}^K n_{\{j,l\}}(k, m) = n$.

To compute the estimate $\hat{f}_{\{j,l\},ALE}(x_j, x_l)$, we first compute an estimate of the uncentered effect $\tilde{f}_{\{j,l\},ALE}(x_j, x_l)$ defined in (8), which is

$$\hat{\tilde{f}}_{\{j,l\},ALE}(x_j, x_l) = \sum_{k=1}^{k_j(x_j)} \sum_{m=1}^{k_l(x_l)} \frac{1}{n_{\{j,l\}}(k,m)} \sum_{\{i: \mathbf{x}_{i,\{j,l\}} \in N_{\{j,l\}}(k,m)\}} \Delta_f^{\{j,l\},k,m}(\mathbf{x}_{i,\setminus\{j,l\}}) \quad (13)$$

for each $(x_j, x_l) \in (z_{0,j}, z_{K,j}] \times (z_{0,l}, z_{K,l}]$. In (13),

$$\begin{aligned} \Delta_f^{\{j,l\},k,m}(\mathbf{x}_{i,\setminus\{j,l\}}) &= [f(z_{k,j}, z_{m,l}, \mathbf{x}_{i,\setminus\{j,l\}}) - f(z_{k-1,j}, z_{m,l}, \mathbf{x}_{i,\setminus\{j,l\}})] \\ &\quad - [f(z_{k,j}, z_{m-1,l}, \mathbf{x}_{i,\setminus\{j,l\}}) - f(z_{k-1,j}, z_{m-1,l}, \mathbf{x}_{i,\setminus\{j,l\}})] \end{aligned} \quad (14)$$

is the second-order finite difference of $f(\mathbf{x}) = f(x_j, x_l, \mathbf{x}_{\setminus\{j,l\}})$ with respect to (x_j, x_l) , evaluated at $\mathbf{x} = (z_{k,j}, z_{m,l}, \mathbf{x}_{i,\setminus\{j,l\}})$. Paralleling (9), we next compute estimates of the ALE main effects of

x_j and x_l for the function $\hat{\hat{f}}_{\{j,l\},ALE}(x_j, x_l)$ and then subtract these from $\hat{\hat{f}}_{\{j,l\},ALE}(x_j, x_l)$ to give an estimate of $\tilde{f}_{\{j,l\},ALE}(x_j, x_l)$:

$$\begin{aligned} \hat{\hat{f}}_{\{j,l\},ALE}(x_j, x_l) &= \hat{\hat{f}}_{\{j,l\},ALE}(x_j, x_l) - \sum_{k=1}^{k_j(x_j)} \frac{1}{n_j(k)} \sum_{\{i: x_{i,j} \in N_j(k)\}} \left[\hat{\hat{f}}_{\{j,l\},ALE}(z_{k,j}, x_{i,l}) - \hat{\hat{f}}_{\{j,l\},ALE}(z_{k-1,j}, x_{i,l}) \right] \\ &\quad - \sum_{m=1}^{k_l(x_l)} \frac{1}{n_l(m)} \sum_{\{i: x_{i,l} \in N_l(m)\}} \left[\hat{\hat{f}}_{\{j,l\},ALE}(x_{i,j}, z_{m,l}) - \hat{\hat{f}}_{\{j,l\},ALE}(x_{i,j}, z_{m-1,l}) \right] \\ &= \hat{\hat{f}}_{\{j,l\},ALE}(x_j, x_l) - \sum_{k=1}^{k_j(x_j)} \frac{1}{n_j(k)} \sum_{m=1}^K n_{\{j,l\}}(k, m) \left[\hat{\hat{f}}_{\{j,l\},ALE}(z_{k,j}, z_{m,l}) - \hat{\hat{f}}_{\{j,l\},ALE}(z_{k-1,j}, z_{m,l}) \right] \\ &\quad - \sum_{m=1}^{k_l(x_l)} \frac{1}{n_l(m)} \sum_{k=1}^K n_{\{j,l\}}(k, m) \left[\hat{\hat{f}}_{\{j,l\},ALE}(z_{k,j}, z_{m,l}) - \hat{\hat{f}}_{\{j,l\},ALE}(z_{k,j}, z_{m-1,l}) \right]. \quad (15) \end{aligned}$$

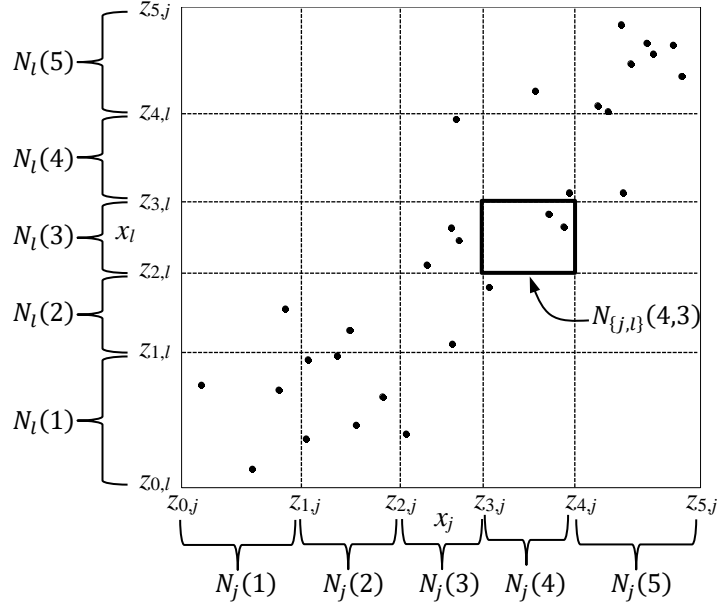


Figure 4. Illustration of the notation used in computing the ALE second-order effect estimator $\hat{\hat{f}}_{\{j,l\},ALE}(x_j, x_l)$ for $K = 5$. The ranges of $\{x_{i,j}; i = 1, 2, \dots, n\}$ and $\{x_{i,l}; i = 1, 2, \dots, n\}$ are each partitioned into 5 intervals, and their Cartesian product forms the grid of rectangular cells $\{N_{\{j,l\}}(k, m) = N_j(k) \times N_l(m); k = 1, 2, \dots, 5; m = 1, 2, \dots, 5\}$. The cell with bold borders is the region $N_{\{j,l\}}(4,3)$. The second-order finite differences $\Delta_f^{\{j,l\},k,m}(\mathbf{x}_{i \setminus \{j,l\}})$ in Eq. (14) for $(k, m) = (4,3)$ are calculated across the corners of this cell. In the inner summation of Eq. (13), these differences are then averaged over the $n_{\{j,l\}}(4,3) = 2$ observations in region $N_{\{j,l\}}(4,3)$.

Finally, paralleling (10), we compute the estimate of $f_{\{j,l\},ALE}(x_j, x_l)$ by subtracting an estimate of $E \left[\hat{\hat{f}}_{\{j,l\},ALE}(X_j, X_l) \right]$ from (15), which gives

$$\begin{aligned}
\hat{f}_{\{j,l\},ALE}(x_j, x_l) &= \hat{\hat{f}}_{\{j,l\},ALE}(x_j, x_l) - \frac{1}{n} \sum_{i=1}^n \hat{\hat{f}}_{\{j,l\},ALE}(x_{i,j}, x_{i,l}) \\
&= \hat{\hat{f}}_{\{j,l\},ALE}(x_j, x_l) - \frac{1}{n} \sum_{k=1}^K \sum_{m=1}^K n_{\{j,l\}}(k, m) \hat{\hat{f}}_{\{j,l\},ALE}(z_{k,j}, z_{m,l}).
\end{aligned} \tag{16}$$

We define ALE plot as plots of the ALE effect estimates $\hat{f}_{j,ALE}(x_j)$ and $\hat{f}_{\{j,l\},ALE}(x_j, x_l)$ versus the predictors involved. ALE plots have substantial computational advantages over PD plot, which we discuss in Section 5.2. In addition, ALE plots can produce reliable estimates of the main and interaction effects in situations where PD plots break down, which we illustrate with examples in the next section.

4. Examples where ALE Plots are Reliable but PD Plots Break Down

Example 1 was introduced in the Section 1. For this example, $d = 2$, $n = 200$, and $\{X_1, X_2\}$ follows a uniform distribution along a segment of the line $x_2 = x_1$ with independent $N(0, 0.05^2)$ variables added to both predictors. Figure 5 shows a scatter plot of X_2 vs. X_1 . The true response was generated according to the noiseless model $Y = X_1 + X_2^2$ for the 200 training observations in Figure 5, to which we fit a tree using the `tree` package of R (Ripley, 2015). The tree was overgrown and then pruned back to have 100 leaf nodes, which was approximately the optimal number of leaf nodes according to a cross-validation error sum of squares criterion. Notice that the optimal size tree is relatively large, because the response here is a deterministic function $X_1 + X_2^2$ of the predictors with no response observation error. The first eight splits of the fitted tree $f(\mathbf{x})$ are also depicted in Figure 5. Figure 6 shows main effect PD plots, M plots, and ALE plots for the full 100-node fitted tree $f(\mathbf{x})$, calculated via (2), (4), and (11)—(12), respectively. For both $j = 1$ and $j = 2$, $\hat{f}_{j,ALE}(x_j)$ is much more accurate than either $\hat{f}_{j,PD}(x_j)$ or $\hat{f}_{j,M}(x_j)$. By inspection of the fitted tree in Figure 5, it is clear why $\hat{f}_{j,PD}(x_j)$ performs so poorly in this example. For small x_1 values like $x_1 \approx 0.2$, the PD plot estimate $\hat{f}_{1,PD}(x_1 \approx 0.2)$ is much higher than it should be, because it is based on the extrapolated values of $f(\mathbf{x})$ in the upper-left corner of the scatter plot in Figure 5, which were substantially overestimated due to the nature of tree splits and the absence of any data in that region. For similar reasons, $\hat{f}_{2,PD}(x_2)$ for small x_2 values is substantially

underestimated because of the extrapolation in the lower-right corner of the scatter plot in Figure 5. In contrast, by avoiding this extrapolation, $\hat{f}_{1,ALE}(x_1)$ and $\hat{f}_{2,ALE}(x_2)$ are still estimated quite accurately and are quite close to the true linear (for x_1) and quadratic (for x_2) effects, as seen in Figures 4(a) and 4(b), respectively.

Also notice that the M plots in Figures 4(a) and 4(b) perform very poorly. As expected, because of the strong correlation between X_1 and X_2 , $\hat{f}_{1,M}(x_1)$ and $\hat{f}_{2,M}(x_2)$ are quite close to each other and are each combinations of the true effects of X_1 and X_2 . In the subsequent examples, we do not further consider M plots.

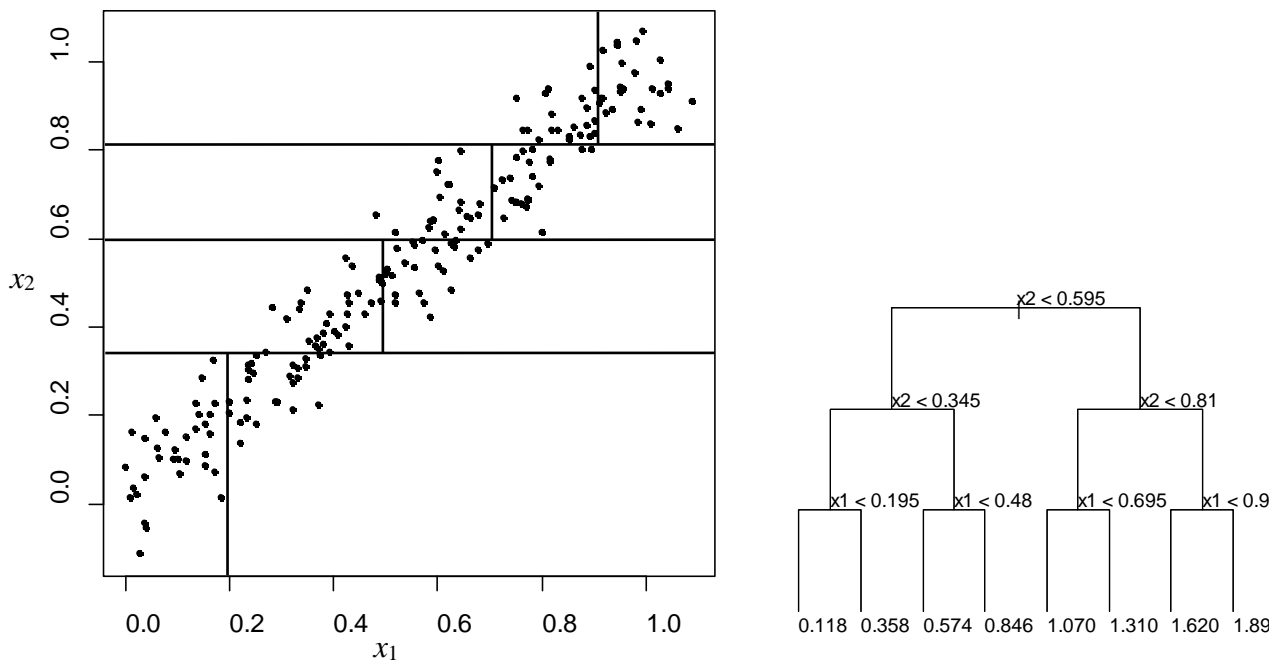


Figure 5. Depiction of the first eight splits in the tree fitted to the Example 1 data. The left panel is a scatterplot of x_2 vs. x_1 showing splits corresponding to the truncated tree in the right panel.

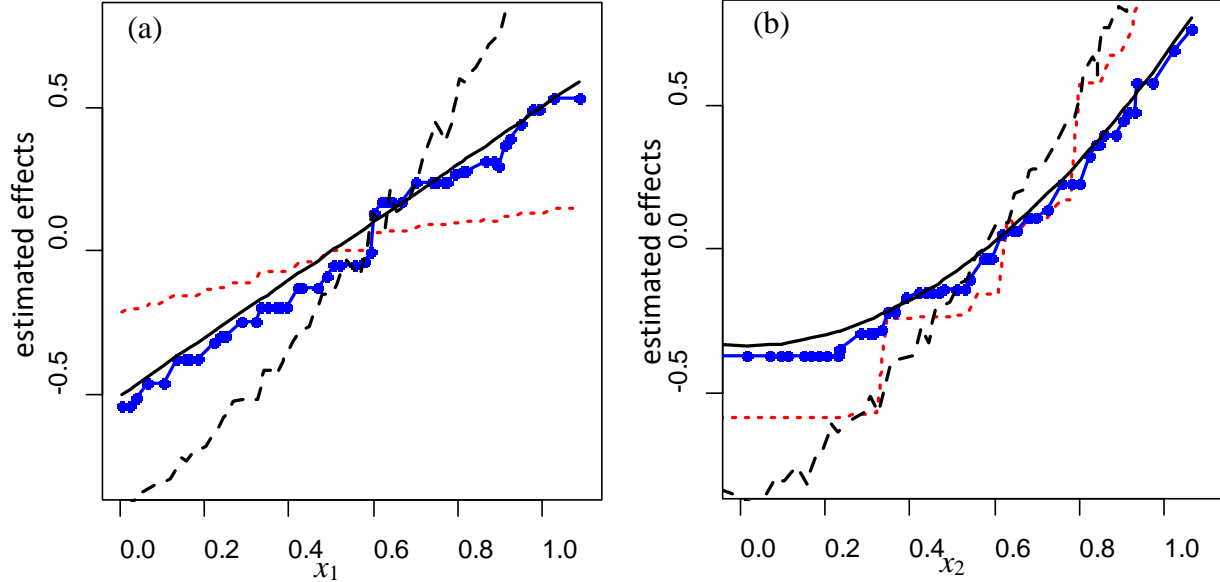


Figure 6. For the tree model fitted to the Example 1 data, plots of $\hat{f}_{j,ALE}(x_j)$ (blue line with bullets), $\hat{f}_{j,PD}(x_j)$ (red dotted line), $\hat{f}_{j,M}(x_j)$ (black dashed line), and the true main effect of x_j (black solid line) for (a) $j = 1$, for which the true effect of x_1 is linear, and (b) $j = 2$, for which the true effect of x_2 is quadratic. For both $j = 1$ and $j = 2$, $\hat{f}_{j,ALE}(x_j)$ is much more accurate than either $\hat{f}_{j,PD}(x_j)$ or $\hat{f}_{j,M}(x_j)$.

Example 2 is a modification of Example 1 having the same $d = 2$, $n = 200$, and $\{X_1, X_2\}$ following a uniform distribution along a segment of the line $x_2 = x_1$ with independent $N(0, 0.05^2)$ variables added to both predictors. However, the true response is now generated as noisy observations according to the model $Y = X_1 + X_2^2 + \varepsilon$ with $\varepsilon \sim N(0, 0.1^2)$, and we fit a neural network model instead of a tree. For the neural network, we used the `nnet` package of R (Venables and Ripley, 2002) with ten nodes in the single hidden layer, a linear output activation function, and a decay/regularization parameter of 0.0001, all of which were chosen as approximately optimal via multiple replicates of 10-fold cross-validation (the cross-validation r^2 for this model varied between 0.965 and 0.975, depending on the data set generated, which is quite close to the theoretical r^2 value of $1 - \text{var}(\varepsilon)/\text{var}(Y) = 0.972$). We repeated the procedure in a Monte Carlo simulation with 50 replicates, where on each replicate we generated a new training data set of 200 observations and refit the neural network model with the same tuning parameters mentioned above. The estimated main effect functions $\hat{f}_{j,ALE}(x_j)$ and $\hat{f}_{j,PD}(x_j)$ (for $j = 1, 2$) over all 50 replicates are shown in Figure 7. For this example too, $\hat{f}_{j,ALE}(x_j)$ is far superior to $\hat{f}_{j,PD}(x_j)$.

On every replicate, $\hat{f}_{1,ALE}(x_1)$ and $\hat{f}_{2,ALE}(x_2)$ are quite close to the true linear and quadratic effects, respectively. In sharp contrast, $\hat{f}_{1,PD}(x_1)$ and $\hat{f}_{2,PD}(x_2)$ are so inaccurate on many replicates that they are of little use in understanding the true effects of X_1 and X_2 .

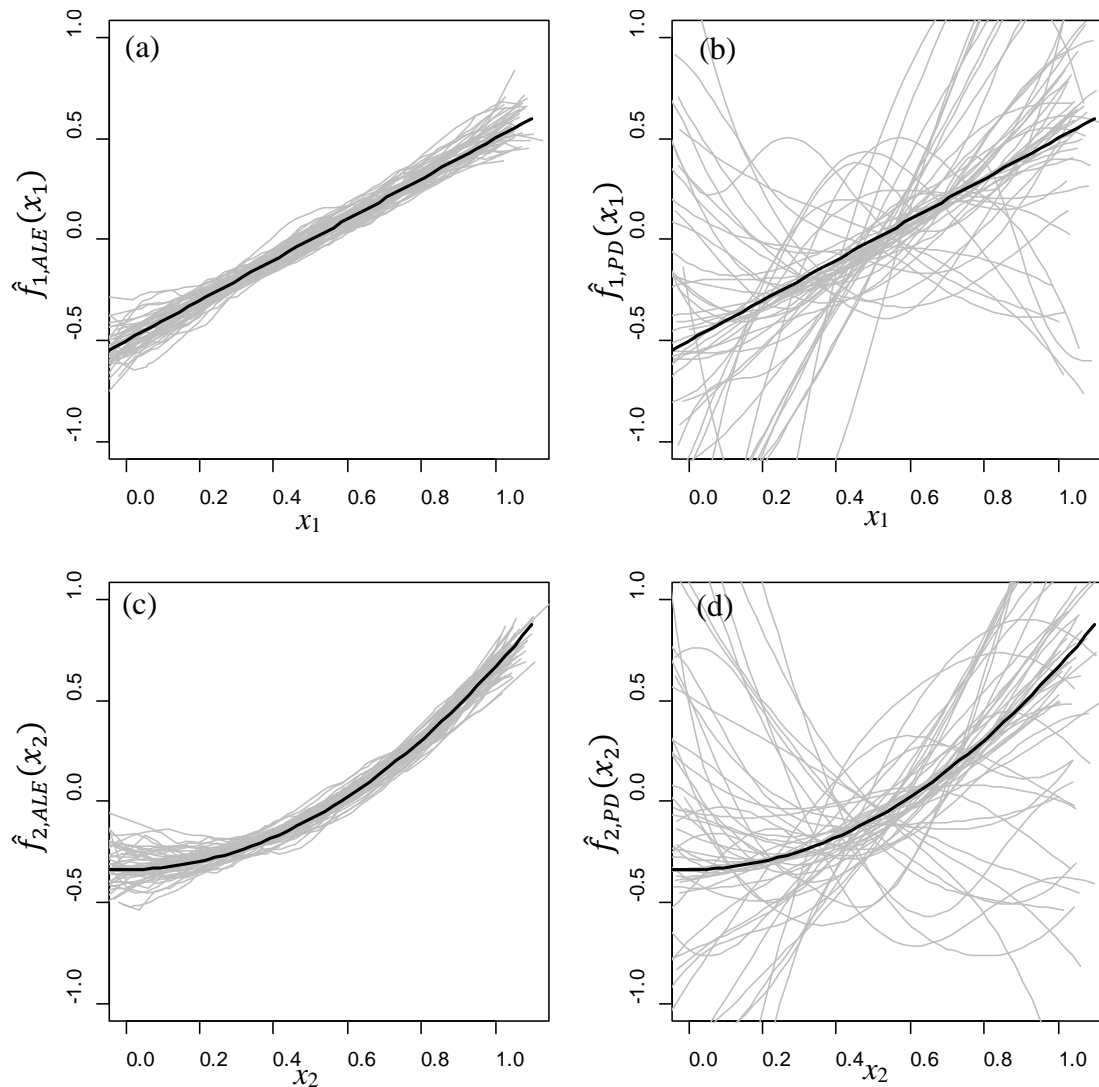


Figure 7. Comparison of (a) $\hat{f}_{1,ALE}(x_1)$, (b) $\hat{f}_{1,PD}(x_1)$, (c) $\hat{f}_{2,ALE}(x_2)$, and (d) $\hat{f}_{2,PD}(x_2)$ for neural network models fitted over 50 Monte Carlo replicates of the Example 2 data. In each panel, the black curve is the true effect function (linear for X_1 and quadratic for X_2), and the gray curves are the estimated effect functions over the 50 Monte Carlo replicates.

5. Discussion

5.1 Paired Differencing and the Unbiasedness of the ALE Effects

The ALE effects have a form of unbiasedness that is desirable. Suppose $f(\mathbf{x}) = \sum_{j=1}^d f_j(x_j)$ is an additive function of the individual predictors. Then it is straightforward to show that the ALE main effects are $f_{j,ALE}(x_j) = f_j(x_j)$ ($j = 1, 2, \dots, d$), up to an additive constant. That is, the ALE effects return the correct additive functions. More generally, the following result states that higher-order ALE effects $f_{J,ALE}(\mathbf{x}_J)$ have a similar unbiasedness.

Additive unbiasedness of ALE plots. Suppose the model is of the form $f(\mathbf{x}) = \sum_{J \subseteq \{1,2,\dots,d\}, |J| \leq k} f_J(\mathbf{x}_J)$ for some $1 \leq k \leq d$. That is, $f(\mathbf{x})$ has interactions of order k , but no higher-order interactions than that. Then for each J with $|J| = k$, $f_{J,ALE}(\mathbf{x}_J) = f_J(\mathbf{x}_J) + \sum_{u \subset J} h_u(\mathbf{x}_u)$ for some lower-order functions $h_u(\mathbf{x}_u)$. That is, the ALE effect $f_{J,ALE}(\mathbf{x}_J)$ returns the correct k -order interaction $f_J(\mathbf{x}_J)$, except for the additive presence of strictly lower-order functions, which do not alter the interpretation of the k -order interaction.

The proof of the additive unbiasedness result follows directly from the decomposition theorem in Appendix B. It also follows that if the functions $\{f_J(\mathbf{x}_J)\}$ in the expression for $f(\mathbf{x})$ are adjusted so that each has no lower-order ALE effects, then $f_{J,ALE}(\mathbf{x}_J) = f_J(\mathbf{x}_J)$ for each $J \subseteq \{1, 2, \dots, d\}$. PD plots have a related unbiasedness property that we discuss below. M plots have no such property. For example, if $f(\mathbf{x}) = \sum_{j=1}^d f_j(x_j)$, and the predictors are dependent, then each $f_{j,M}(x_j)$ may be a combination of the main effects of many predictors. As discussed previously, this can be viewed as the omitted variable bias in regression, whereby a regression of Y on (say) X_1 , omitting a correlated nuisance variable X_2 , will bias the effect of X_1 on Y if Y also depends on X_2 .

The mechanism by which ALE plots avoid this omitted nuisance variable bias is illustrated in Figure 8, for the same example depicted in Figures 1, 2, and 5. First note that the M plot effect is biased because $f_{1,M}(x_1)$ averages the *global* effect $f(x_1, X_2)$ with respect to the conditional distribution of $X_2 | X_1 = x_1$ (see (3) and (4)). For example, for $f(\mathbf{x}) = x_1 + x_2^2$ considered in Figure 6, the averaged global effect for the M plot is $f_{1,M}(x_1) = E[f(X_1, X_2) | X_1 = x_1] = x_1 +$

$E[X_2^2|X_1 = x_1] \neq x_1$, which is biased by the functional dependence of $f(\mathbf{x})$ on the correlated nuisance variable X_2 . In contrast to averaging the global effect, the ALE effect $f_{1,ALE}(x_1)$ estimated via (11)—(12) averages the *local* effect represented by the paired differences $f(z_{k,1}, x_{i,2}) - f(z_{k-1,1}, x_{i,2})$ in (11). As illustrated in Figure 8, this paired differencing is what blocks out the effect of the correlated nuisance variable X_2 . Continuing the $f(\mathbf{x}) = x_1 + x_2^2$ example, the paired differences $f(z_{k,1}, x_{i,2}) - f(z_{k-1,1}, x_{i,2}) = (z_{k,1} + x_{i,2}^2) - (z_{k-1,1} + x_{i,2}^2) = z_{k,1} - z_{k-1,1}$ for the ALE plot completely block out the effect of X_2 , so that the accumulated local effect $\sum_{k=1}^{k_1(x_1)} [z_{k,1} - z_{k-1,1}] = x_1 + \text{constant}$ is correct.

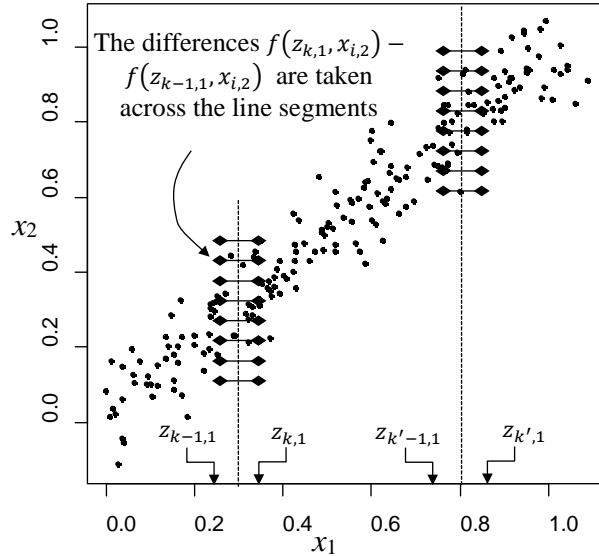


Figure 8. Illustration of how, when estimating $f_{1,ALE}(x_1)$, the differences $f(z_{k,1}, x_{i,2}) - f(z_{k-1,1}, x_{i,2})$ and $f(z_{k',1}, x_{i,2}) - f(z_{k'-1,1}, x_{i,2})$ in (11) are paired differences that block out the nuisance variable X_2 . Here, $k = k_1(0.3)$ and $k' = k_1(0.8)$.

Multiplicative unbiasedness of ALE plots for independent subsets of predictors. Suppose the model is of the form $f(\mathbf{x}) = f_J(\mathbf{x}_J)f_{\setminus J}(\mathbf{x}_{\setminus J})$ for some $J \subset \{1, 2, \dots, d\}$ with the corresponding subsets \mathbf{X}_J and $\mathbf{X}_{\setminus J}$ of predictors independent of each other. In this case it is straightforward to show that the ALE $|J|$ -order interaction effect of \mathbf{x}_J is $f_{J,ALE}(\mathbf{x}_J) = f_J(\mathbf{x}_J)E[f_{\setminus J}(\mathbf{X}_{\setminus J})] + \sum_{u \subset J} h_u(\mathbf{x}_u)$ for some lower-order functions $h_u(\mathbf{x}_u)$. That is, the ALE $|J|$ -order interaction effect $f_{J,ALE}(\mathbf{x}_J)$ returns the correct function $f_J(\mathbf{x}_J)$, except for a multiplicative constant $E[f_{\setminus J}(\mathbf{X}_{\setminus J})]$ and the additive presence of strictly lower-order functions.

Comparison to PD plots. PD plots also have the same additive and multiplicative unbiasedness properties as ALE plots. Moreover, for $f(\mathbf{x}) = f_J(\mathbf{x}_J)f_{\setminus J}(\mathbf{x}_{\setminus J})$, PD plots have multiplicative unbiasedness (up to a multiplicative constant) even when \mathbf{X}_J and $\mathbf{X}_{\setminus J}$ are dependent (Hastie, et al., 2009). Although it is probably desirable to have multiplicative unbiasedness when \mathbf{X}_J and $\mathbf{X}_{\setminus J}$ are independent, it is unclear whether multiplicative unbiasedness is desirable if \mathbf{X}_J and $\mathbf{X}_{\setminus J}$ are dependent.

For example, suppose $f(\mathbf{x}) = x_1x_2$ with X_1 ($J = 1$) and X_2 ($\setminus J = 2$) standard normal random variables with correlation coefficient ρ . It is straightforward to show that $f_{\{1,2\},ALE}(x_1, x_2) = x_1x_2 - \rho(x_1^2 + x_2^2 - 1)$, $f_{1,ALE}(x_1) = \rho(x_1^2 - 1)$, and $f_{2,ALE}(x_2) = \rho(x_2^2 - 1)$, compared to $f_{\{1,2\},PD}(x_1, x_2) = x_1x_2$, $f_{1,PD}(x_1) = 0$, and $f_{2,PD}(x_2) = 0$. Because of the strong interaction, it is essential to look at the second-order interaction effects in order to understand the functional dependence of $f(\cdot)$ on the predictors. Both $f_{\{1,2\},ALE}(x_1, x_2)$ and $f_{\{1,2\},PD}(x_1, x_2)$ yield correct unbiased assessments of the interaction, up to lower-order functions of the individual predictors. Regarding the main effects, however, the picture is more ambiguous. First, it is important to note that with a strong interaction and dependent predictors, it is unclear whether the main effects are even meaningful. And it is equally unclear whether the PD main effect $f_{1,PD}(x_1) = 0$ is any more or less meaningful than the ALE main effect $f_{1,ALE}(x_1) = \rho(x_1^2 - 1)$. On the surface, it may appear that $f_{1,PD}(x_1) = 0$ is a more revealing value for the main effect of x_1 . This would be probably be true if X_1 and X_2 were independent, but in this case $f_{1,PD}(x_1) = f_{1,ALE}(x_1) = 0$ would be in agreement. However, the situation is murkier with dependent predictors. The local effect $\partial f(\mathbf{x})/\partial x_1 = x_2$ of x_1 depends strongly on the value of x_2 , in that it is amplified for larger $|x_2|$ and changes sign if x_2 changes sign. Thus, if ρ is large and positive, the local effect of x_1 is positive for $x_1 > 0$ and negative for $x_1 < 0$, which is the local effect of a quadratic relationship. In this case one might argue that the quadratic $f_{1,ALE}(x_1) = \rho(x_1^2 - 1)$ is more revealing than $f_{1,PD}(x_1) = 0$. However, we emphasize that the debate is largely academic, because when strong interactions are present the lower-order effects should not be interpreted in a vacuum.

5.2 Computational Advantages of ALE Plots and a Larger Data Example

For general supervised learning models $f(\mathbf{x})$, ALE plots have an enormous computational advantage over PD plots. Suppose we want to compute $\hat{f}_{J,ALE}(\mathbf{x}_J)$ for one subset $J \subseteq \{1, 2, \dots, d\}$ over a grid in the \mathbf{x}_J -space with K discrete locations for each variable. Computation of $\hat{f}_{J,ALE}(\mathbf{x}_J)$ over this grid requires a total of $2^{|J|} \times n$ evaluations of the supervised learning model $f(\mathbf{x})$ (see (11)—(16) or (C1) for $|J| > 2$). In comparison, computation of $\hat{f}_{J,PD}(\mathbf{x}_J)$ over this grid requires a total of $K^{|J|} \times n$ evaluations of $f(\mathbf{x})$. For example, for $K = 50$, PD main effects and second-order interaction effects require, respectively, 25 and 625 times more evaluations of $f(\mathbf{x})$ than the corresponding ALE effects. Moreover, as we discuss in Appendix D, the evaluations of $f(\mathbf{x})$ can be easily vectorized in R by appropriately calling the `predict` function that is built into most supervised learning packages in R.

Also notice that the number of evaluations of $f(\mathbf{x})$ for ALE plots does not depend on K , which is convenient. As n increases, the observations become denser, in which case we may want the fineness of the discretization to increase as well. If we choose $K^{|J|} \propto n$ (which results in the same average number of observations per cell as n increases), then the number of evaluations of $f(\mathbf{x})$ is $O(n)$ for ALE plots versus $O(n^2)$ for PD plots.

Income Data Example. We now show an example with a real, larger data set. The data are a compilation of the 1994 US Census data from the University of California Irvine Machine learning repository at <http://archive.ics.uci.edu/ml/datasets/Census+Income>. There are $n = 30,162$ cases in the training data set (after removing cases with missing data), and each case represents a person. The response is the binary categorical variable indicating whether a person made more than \$50k income in 1994. The $d = 12$ predictor variables are: age (x_1 , numerical); working class (x_2 , categorical with 8 categories); education level (x_3 , treated as numerical: 1 = preschool, 2 = 1st—4th grade, 3 = 5th-6th grade, 4 = 7th-8th grade, 5 = 9th grade, 6 = 10th grade, 7 = 11th grade, 8 = 12th grade, 9 = high school graduate, 10 = some college, 11 = vocational associates degree, 12 = academic associates degree, 13 = bachelor's degree, 14 = master's degree, 15 = professional degree,

16 = doctorate degree); marital status (x_4 , categorical with 7 categories); occupation (x_5 , categorical with 13 categories); relationship status (x_6 , categorical with 6 categories); race (x_7 , categorical with 5 categories) sex (x_8 , categorical with 2 categories); capital gains (x_9 , numerical); capital loss (x_{10} , numerical); hours-per-week spent working (x_{11} , numerical); and native country (x_{12} , categorical with 41 categories). We fit a boosted tree using the R **gbm** package (Ridgeway, 2015) with parameters `shrinkage = 0.02` and `interaction.depth = 3`, for which the optimal number of trees (determined via 10-fold cross-validation) was 6,000. As $f(\mathbf{x})$, we used the log-odds of the predicted probability that a person makes over \$50k from the fitted boosted tree. Figure 9 shows the ALE main effect plots for the age, education level, and hours-per-week predictors and the ALE second-order interaction plot $\hat{f}_{\{1,11\},ALE}(x_1, x_{11})$ for age and hours-per-week. We used $K = 500$ for the main effects plots and $K = 50$ for the interaction plot.

Regarding computational expense, we implemented the preceding ALE and PD plots using our R package **ALEPlot** on a Windows™ laptop with 8-core Intel(R) Core(TM) i7-4712HQ CPU @ 2.30 GHz processor. The ALE main effects plots took about 9 seconds each, and the ALE second-order interaction plot took about 15 seconds. In comparison, the PD main effects plots took about 9 minutes each with $K = 100$, and the PD interaction plot took about 35 minutes with $K = 20$. The PD plot computational expense is proportional to K for main effects and to K^2 for second-order interactions, whereas the ALE plot computational expense is largely independent of K . For this example, the PD plots were nearly identical to the ALE plots in Figure 9 and are not shown here. However, the ALE plots were orders of magnitude faster to compute (15 seconds vs. 35 minutes for the interaction plot).

Regarding interpretation of the results, the ALE main effects plots in Figure 9 have clear interpretations. The probability of earning more than \$50k (*i*) gradually increases with age until it peaks around 50 years and then gradually declines; (*ii*) monotonically increases with education level, with the largest jumps occurring when going from Associates to Bachelor's, from Bachelor's to Master's, and from Master's to Ph.D./Professional degrees; and (*iii*) monotonically increases

with hours per week worked up until about 50 hours per week, with the steepest increases between roughly 30—50 hours per week.

The ALE second-order {age, hours per week} interaction plot in Figure 9 also reveals an interesting relationship. Consider the increased probability of earning more than \$50k that is associated with increasing hours per week from 35 to 80. From the interaction plot, the amount that this probability increases depends on age. For 25-year-olds the increase in probability is larger than for 75-year-olds (because $\hat{f}_{\{1,11\},ALE}(x_1, x_{11})$ increases by 0.3 units for 25-year-olds increasing hours per week from 35 to 80, but it decreases by 0.5 units for 75-year-olds increasing hours per week by the same amount). Perhaps this is because 75-year-olds who work so many hours may be more compelled to do so for financial reasons than 25-year-olds (or perhaps there are other explanations).

A word of caution is in order on interpreting the ALE interaction plots. By definition, $\hat{f}_{\{1,11\},ALE}(x_1, x_{11})$ has no x_1 or x_{11} ALE main effects, because they are subtracted from it. Thus, the fact that $\hat{f}_{\{1,11\},ALE}(x_1, x_{11})$ *decreases* by 0.5 for 75-year-olds going from 35 to 80 hours per week does not imply that such an increase in hours per week is associated with decrease in the probability of a 75-year-old earning more than \$50k. To gauge this, we must look at whether $\hat{f}_{11,ALE}(x_{11}) + \hat{f}_{\{1,11\},ALE}(75, x_{11})$ increases or decreases when going from $x_{11} = 35$ to $x_{11} = 80$ hours per week. From Figure 9 this still increases by about 0.6 units for 75-year-olds, so at any age, increasing hours per week worked is associated with an increase in the probability of earning more than \$50k.

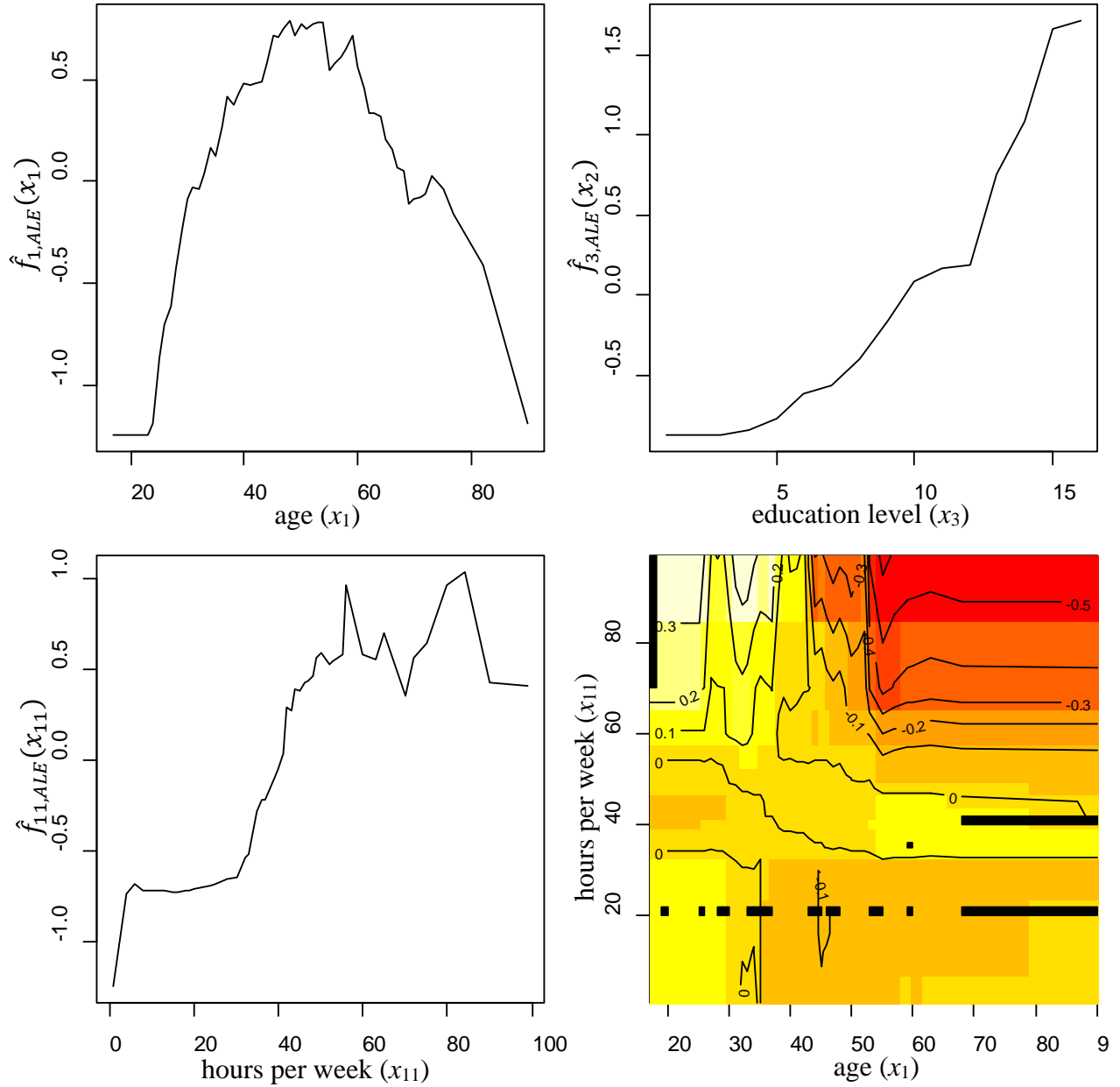


Figure 9. For the income data example with boosted tree log-odds for $f(\mathbf{x})$, ALE main effect plots for age, education level, and hours per week (top panels and bottom left panel) and ALE second-order interaction plot for {age, hours per week} (bottom right panel). The black rectangles in the interaction plot indicate empty cells, into which none of the training observations fell.

5.3 Relation to Functional ANOVA with Dependent Inputs

In the context of the closely-related problem of functional ANOVA with dependent input/predictor variables, the extrapolation issue that motivated ALE plots has been previously considered. Hooker (2007) proposed a functional ANOVA decomposition of $f(\mathbf{x})$ into component functions $\{f_{J,ANOVA}(\mathbf{x}_J): J \subseteq \{1, 2, \dots, d\}\}$ by adopting the Stone (1994) approach of using weighted integrals in the function approximation optimality criterion and in the component function orthogonality constraints. Hooker (2007) used $p_{\{1, 2, \dots, d\}}(\mathbf{x})$ as a weighting function, which indirectly avoids extrapolation of $f(\mathbf{x})$ in regions in which there are no training observations, because any such extrapolations are assigned little or no weight. The resulting ANOVA component functions are *hierarchically orthogonal* under the correlation inner product, in the sense that $f_{J,ANOVA}(\mathbf{X}_J)$ and $f_{u,ANOVA}(\mathbf{X}_u)$ are uncorrelated when $u \subset J$. However, $f_{J,ANOVA}(\mathbf{X}_J)$ and $f_{u,ANOVA}(\mathbf{X}_u)$ are not uncorrelated for general $u \neq J$.

The orthogonality-like property for the ALE decomposition mentioned in Remark 1 and described in more detail in Appendix B is not true orthogonality (at least, we have not found an inner product for which it is), although it is closely related. For each $J \subseteq \{1, 2, \dots, d\}$, let $\mathcal{H}_J(\cdot)$ denote the operator that maps a function f to its ALE effect $f_{J,ALE}$, i.e., such that $f_{J,ALE} = \mathcal{H}_J(f)$ (see Appendix B for details). The collection of operators $\{\mathcal{H}_J: J \subseteq \{1, 2, \dots, d\}\}$ behaves like a collection of operators that project onto orthogonal subspaces of an inner product space. Namely, if " \circ " denotes the composite function operator, then $\mathcal{H}_u \circ \mathcal{H}_J(f) = 0$ for $u \neq J$, and $\mathcal{H}_u \circ \mathcal{H}_u(f) = \mathcal{H}_u(f)$.

For the purpose of visualizing the effects of the predictors on black box supervised learning models, the correlation orthogonality in other functional ANOVA decompositions may be less relevant and useful than the ALE pseudo-orthogonality. As discussed in Roosen (1995), if the predictors are dependent, it may even be preferable to artificially impose a product $p_{\{1, 2, \dots, d\}}(\mathbf{x})$ in the functional ANOVA decomposition to avoid conflating direct and indirect effects of a predictor, and this will typically result in ANOVA component functions that are no longer uncorrelated. For

example, suppose $f(\mathbf{x}) = x_1 + x_2$ with X_1 and X_2 correlated. Any functional ANOVA decomposition that gives uncorrelated main effects will not give the correct main effects $f_1(x_1) = x_1$ and $f_2(x_2) = x_2$ that are needed to understand the true functional dependence of $f(\mathbf{x})$ on x_1 and x_2 , whereas ALE plots and PD plots will. Functional ANOVA can be coerced into producing the correct main effects $f_{1,ANOVA}(x_1) = x_1$ and $f_{2,ANOVA}(x_2) = x_2$ by artificially imposing a product distribution $p_{\{1,2\}}(\mathbf{x}) = p_1(x_1)p_2(x_2)$, but then the ANOVA component functions will obviously be correlated. Moreover, artificially imposing a product $p_{\{1,2,\dots,d\}}(\mathbf{x})$ in functional ANOVA still leaves the extrapolation problem that motivates ALE plots and the work of Hooker (2007).

In addition, practical implementation is far more cumbersome for functional ANOVA decompositions than for ALE (or PD) plots for multiple reasons. First, $p_{\{1,2,\dots,d\}}(\mathbf{x})$ must be estimated in the functional ANOVA approach of Hooker (2007), which is problematic in high-dimensions. In contrast, the ALE effect estimates (11)—(16) involve summations over the training data but require no estimate of $p_{\{1,2,\dots,d\}}(\mathbf{x})$. Second, ALE plots can be computed sequentially (main effects first, followed by second-order interactions, followed by third-order interactions, etc., each computed one-at-a-time) using the straightforward and computationally efficient summations. In contrast, the functional ANOVA component functions must all be solved simultaneously, which requires the solution of a complex system of equations. Follow-up work in Li and Rabitz (2012), Chastaing, et al. (2012), and Rahman (2014) improved the solution techniques, sometimes restricting the component ANOVA functions to be expansions in basis functions such as polynomials and splines, but these are more restrictive (perhaps negating the benefits of fitting a black box supervised learning model in the first place), as well as more cumbersome and computationally expensive than ALE plots.

6. Conclusions

For visualizing the effects of the predictor variables in black box supervised learning models, PD plots are the most widely used method. The ALE plots that we have proposed in this paper are

an alternative that has two important advantages over PD plots. First, by design, ALE plots avoid the extrapolation problem that can render PD plots unreliable when the predictors are highly correlated (see Figures 6 and 7). Second, ALE plots are substantially less computationally intensive than PD plots, requiring only $2^{|J|} \times n$ evaluations of the supervised learning model $f(\mathbf{x})$ to compute each $\hat{f}_{J,ALE}(\mathbf{x}_J)$, compared to $K^{|J|} \times n$ evaluations to compute each $\hat{f}_{J,PD}(\mathbf{x}_J)$. In light of this, we suggest that ALE plots should be adopted as a standard visualization component in supervised learning software. We have also provided, as supplementary material, an R package **ALEPlot** to implement the ALE plots.

Acknowledgments

This research was supported by XXX Grant #XXX, which the authors gratefully acknowledge.

References

- Chambers, J. M. and Hastie, T. J., (1992), *Statistical Models in S*, Wadsworth & Brooks/Cole, Pacific Grove, CA.
- Chastaing, G., Gamboa, F. and Prieur, C., (2012), "Generalized Hoeffding-Sobol decomposition for dependent variables - Application to sensitivity analysis," *Electronic Journal of Statistics*, 6, pp. 2420–2448.
- Cleveland, W. S., (1993), *Visualizing Data*, Hobart Press, Summit, NJ.
- Cook, D. R., (1995), "Graphics for Studying the Net Effects of Regression Predictors," *Statistica Sinica*, 5, 689—708.
- Friedman, J. H., (2001), "Greedy function approximation: A gradient boosting machine," *Annals of Statistics*, 29(5), pp. 1189–1232.
- Goldstein, A., Kapelner, A., Bleich, J., and Pitkin, E., (2014), "Peeking Inside the Black Box: Visualizing Statistical Learning with Plots of Individual Conditional Expectation," *Journal of Computational & Graphical Statistics*, in press.
- Hastie, T., Tibshirani, R., and Friedman, J., (2009), *The elements of statistical learning*, Springer, New York.
- Hooker, G., (2007), "Generalized functional ANOVA diagnostics for high dimensional functions of dependent variables," *Journal of Computational and Graphical Statistics*, 16, pp. 709–732.

- Li, G. and Rabitz, H., (2012), "General formulation of HDMR component functions with independent and correlated variables," *Journal of Mathematical Chemistry*, 50, pp. 99–130.
- Rahman, S., (2014), "A Generalized ANOVA Dimensional Decomposition for Dependent Probability Measures," *SIAM/ASA Journal of Uncertainty Quantification*, 2, pp. 670—697.
- Ridgeway, G., with contributions from others (2015). "gbm: Generalized Boosted Regression Models. R package version 2.1.1," <http://CRAN.R-project.org/package=gbm>
- Ripley, B. D. (2015). "tree: Classification and Regression Trees. R package version 1.0-36," <http://CRAN.R-project.org/package=tree>.
- Roosen, C. B., (1995), *Visualization and Exploration of High-Dimensional Functions Using the Functional Anova Decomposition*, PhD thesis, Stanford University.
- Stone, C. J., (1994), "The use of polynomial splines and their tensor products in multivariate function estimation," *Annals of Statistics*, 22, pp. 118–171.
- Venables, W. N. and Ripley, B. D. (2002) *Modern Applied Statistics with S. Fourth Edition*. Springer, New York. ISBN 0-387-95457-0.

Appendix A. ALE Plot Definition for Higher-Order Effects

Although we do not envision ALE plots being commonly used to visualize third-and-high-order effects, the notion of higher-order ALE effects is required to fully understand what the ALE plots are estimating and, in particular, to understand the ALE decomposition theorem in Appendix B. The latter was used to derive the additive unbiasedness results in Section 5.1.

Let $\mathbf{X}_J = (X_j: j \in J)$ denote a subset of predictors and $\mathbf{X}_{\setminus J}$ their complement in the full set $\mathbf{X} = (X_j: j = 1, 2, \dots, d)$, where $J \subseteq D \equiv \{1, 2, \dots, d\}$ is the subset of variable indices. As in Section 2, we define the ALE functions $f_{J,ALE}(\mathbf{x}_J)$ for the case of differentiable $f(\cdot)$, noting that the sample estimates $\hat{f}_{J,ALE}(\mathbf{x}_J)$ defined in Appendix C apply to either differentiable or nondifferentiable $f(\cdot)$. Below, we mention how to extend the definition of $f_{J,ALE}(\mathbf{x}_J)$ to nondifferentiable $f(\cdot)$ analogous to Remark 2 in Section 2. Let $f^J(\mathbf{x}_J, \mathbf{x}_{\setminus J}) \equiv \partial^{|\mathbf{J}|} f(\mathbf{x}_J, \mathbf{x}_{\setminus J}) / \partial \mathbf{x}_J$ denote the $|\mathbf{J}|$ -order partial derivative of $f(\mathbf{x}_J, \mathbf{x}_{\setminus J})$ with respect to $(x_j: j \in J)$. For example, if $J = \{3,4\}$, then $f^J(\mathbf{x}_J, \mathbf{x}_{\setminus J}) \equiv \partial^2 f(x_3, x_4, \mathbf{x}_{\setminus J}) / \partial x_3 \partial x_4$. Let $\mathbf{z}_0 = (z_{0,1}, z_{0,2}, \dots, z_{0,d})$ be approximate lower bounds for each

element of (X_1, X_2, \dots, X_d) , as defined in Section 2, and let $\mathbf{z}_{0,J} = (z_{0,j}: j \in J)$ be the subset of elements with indices in J .

We first generalize the definition of the uncentered ALE effects $f_{j,ALE}(x_j)$ and $\tilde{f}_{\{j,l\},ALE}(x_j, x_l)$ to general $J \subseteq D$. Consider the operator \mathcal{L}_J that maps a differentiable function $g: \mathbb{R}^d \mapsto \mathbb{R}$ onto another function $\mathcal{L}_J(g): \mathbb{R}^d \mapsto \mathbb{R}$ defined via

$$\begin{aligned} \mathcal{L}_J(g)(\mathbf{x}_J) &\equiv \int_{\mathbf{z}_J \leq \mathbf{x}_J} E[g^J(\mathbf{X}_J, \mathbf{X}_{\setminus J}) | \mathbf{X}_J = \mathbf{z}_J] d\mathbf{z}_J \\ &= \int_{\mathbf{z}_J \leq \mathbf{x}_J} \int p_{\setminus J|J}(\mathbf{x}_{\setminus J} | \mathbf{z}_J) g^J(\mathbf{z}_J, \mathbf{x}_{\setminus J}) d\mathbf{x}_{\setminus J} d\mathbf{z}_J, \end{aligned} \quad (\text{A1})$$

where the notation $\mathbf{z}_J \leq \mathbf{x}_J$ means that the integration is over the $|J|$ -dimensional rectangle that is the Cartesian product of $\{(z_{0,j}, x_j): j \in J\}$. Note that if we substitute $g = f$ in (A1) for the special case $J = \{j, l\}$, (A1) reduces to $\tilde{f}_{\{j,l\},ALE}(x_j, x_l)$ in (8). In (A1) we have written $\mathcal{L}_J(g)$ as a function of only \mathbf{x}_J to make explicit the fact that it only depends on \mathbf{x}_J . However, it could be viewed as a function of $\mathbf{x} \in \mathbb{R}^d$, defined as its extension from $\mathbb{R}^{|J|}$ to \mathbb{R}^d . For $J = \emptyset$ (the empty set of indices), $\mathcal{L}_\emptyset(g)$ is defined as $E[g(\mathbf{X})] = \int p_D(\mathbf{x}) g(\mathbf{x}) d\mathbf{x}$, the marginal mean of $g(\mathbf{X})$; and for $J = D$ (the complete set of indices), $\mathcal{L}_D(g)(\mathbf{x})$ is defined as $\int_{\mathbf{z} \leq \mathbf{x}} g^D(\mathbf{z}) d\mathbf{z}$.

We will define the ALE $|J|$ -order effect of \mathbf{x}_J on f , which we denote by $f_{J,ALE}$, as a centered version of the function $\mathcal{L}_J(f)$, analogous to how $f_{j,ALE}(x_j)$ and $f_{\{j,l\},ALE}(x_j, x_l)$ were obtained by centering $\tilde{f}_{j,ALE}(x_j)$ and $\tilde{f}_{\{j,l\},ALE}(x_j, x_l)$ in Section 2. For general J , $\mathcal{L}_J(f)$ is comprised of the desired $f_{J,ALE}$, plus lower-order effect functions that are related to f evaluated at the lower boundaries of the rectangular integration region in (A1). Loosely speaking, our strategy is to sequentially subtract the lower-order effects from $\mathcal{L}_J(f)$ to obtain $f_{J,ALE}$.

More formally, let the symbol \circ denote the composition of two operators. For $|J| = 0$ (i.e., $J = \emptyset$), we define the zero-order ALE effect for $f(\cdot)$ as

$$f_{\emptyset,ALE} \equiv \mathcal{H}_\emptyset(f) \equiv \mathcal{L}_\emptyset(f), \quad (\text{A2})$$

a constant that does not depend on \mathbf{x} and that represents the marginal mean $E[f(\mathbf{X})]$ of the function $f(\mathbf{X})$. For $1 \leq |J| < d$, we define the $|J|$ -order effect of \mathbf{x}_J on f as

$$f_{J,ALE}(\mathbf{x}_J) \equiv \mathcal{H}_J(f)(\mathbf{x}_J) \equiv [(I - \mathcal{L}_\emptyset) \circ (I - \sum_{v \subset J, |v|=1} \mathcal{L}_v) \circ (I - \sum_{v \subset J, |v|=2} \mathcal{L}_v) \circ \dots \circ (I - \sum_{v \subset J, |v|=|J|-1} \mathcal{L}_v) \circ \mathcal{L}_J](f)(\mathbf{x}_J), \quad (\text{A3})$$

where I denotes the identity operator, i.e., $I(g) = g$ for a function $g: \mathbb{R}^d \mapsto \mathbb{R}$. The rightmost term in the composite operator \mathcal{H}_J defined in (A3) is just \mathcal{L}_J ; the next rightmost term $(I - \sum_{v \subset J, |v|=J-1} \mathcal{L}_v)$ serves to subtract all of the interactions effects of order $|J| - 1$ from the result $\mathcal{L}_J(f)$ of the previous operation; the next rightmost term $(I - \sum_{v \subset J, |v|=J-2} \mathcal{L}_v)$ serves to subtract all of the interaction terms of order $|J| - 2$ from the result $(I - \sum_{v \subset J, |v|=J-1} \mathcal{L}_v) \circ \mathcal{L}_J(f)$ of the previous operation; and so on. In other words, proceeding from right-to-left, (A3) iteratively subtracts the effects of smaller and smaller order, until the final operator $(I - \mathcal{L}_\emptyset)$ is encountered, which subtracts the zero-order effect from the result of the previous operation. Collectively, these composite operations serve to properly (in the sense of the decomposition theorem in Appendix B) subtract from $\mathcal{L}_J(f)$ all lower-order effects when forming $f_{J,ALE}$. Finally, for $J = D$, we define $f_{D,ALE}(\mathbf{x})$ as the residual error

$$f_{D,ALE}(\mathbf{x}) \equiv \mathcal{H}_D(f)(\mathbf{x}) \equiv [I - \sum_{v \subset D} \mathcal{H}_v](f)(\mathbf{x}). \quad (\text{A4})$$

For the special cases $J = j$ ($|J| = 1$) and $J = \{j, l\}$ ($|J| = 2$), (A3) reduces to $f_{j,ALE}(x_j)$ and $f_{\{j,l\},ALE}(x_j, x_l)$ from (7) and (10), respectively. That is, for $J = j$,

$$\begin{aligned} f_{j,ALE}(x_j) &= [(I - \mathcal{L}_\emptyset) \circ \mathcal{L}_j](f)(x_j) = \mathcal{L}_j(f)(x_j) - \mathcal{L}_\emptyset \circ \mathcal{L}_j(f)(x_j) \\ &= \mathcal{L}_j(f)(x_j) - E[\mathcal{L}_j(f)(X_j)] = \tilde{f}_{j,ALE}(x_j) - E[\tilde{f}_{j,ALE}(X_j)], \end{aligned}$$

which is the same as (7). For $J = \{j, l\}$,

$$\begin{aligned} f_{\{j,l\},ALE}(x_j, x_l) &= [(I - \mathcal{L}_\emptyset) \circ (I - \mathcal{L}_j - \mathcal{L}_l) \circ \mathcal{L}_{\{j,l\}}](f)(x_j, x_l) \\ &= (I - \mathcal{L}_\emptyset) \circ [\mathcal{L}_{\{j,l\}}(f)(x_j, x_l) - \mathcal{L}_j \circ \mathcal{L}_{\{j,l\}}(f)(x_j) - \mathcal{L}_l \circ \mathcal{L}_{\{j,l\}}(f)(x_l)] \\ &= \mathcal{L}_{\{j,l\}}(f)(x_j, x_l) - \mathcal{L}_j \circ \mathcal{L}_{\{j,l\}}(f)(x_j) - \mathcal{L}_l \circ \mathcal{L}_{\{j,l\}}(f)(x_l) \\ &\quad - E[\mathcal{L}_{\{j,l\}}(f)(X_j, X_l) - \mathcal{L}_j \circ \mathcal{L}_{\{j,l\}}(f)(X_j) - \mathcal{L}_l \circ \mathcal{L}_{\{j,l\}}(f)(X_l)], \end{aligned}$$

which is the same as (10).

The definition (A1) of $\mathcal{L}_J(f)$ assumes differentiability of $f(\cdot)$. For nondifferentiable $f(\cdot)$ like regression trees, the definition could be modified as described in Remark 2 of Section 2. This would involve replacing the derivative $f^J(\mathbf{z}_J, \mathbf{x}_{\setminus J})$ by an appropriate finite difference and replacing the outer integration by a finite summation over the same increments used in the finite differences. Taking the limit as the increments approach zero would extend the definitions of $\mathcal{L}_J(f)$ and $f_{J,ALE}(\mathbf{x}_J)$ to nondifferentiable $f(\cdot)$.

Appendix B. ALE Decomposition Theorem and Some Properties of \mathcal{L}_J and \mathcal{H}_J

We first state some properties of \mathcal{L}_J and \mathcal{H}_J , which will be used in the proof of the main result in this appendix. The main result is the ALE decomposition theorem, which states that, in some sense, the ALE plots are estimating the correct quantities.

Properties of \mathcal{L}_J and \mathcal{H}_J : For any two sets of indices $u \subseteq D$ and $J \subseteq D$, we have:

- (i) $\mathcal{L}_u \circ \mathcal{L}_u = \mathcal{L}_u$.
- (ii) $\mathcal{L}_u \circ \mathcal{L}_J = 0$ if $u \not\subseteq J$, i.e., if u contains at least one index that is not in J .
- (iii) \mathcal{L}_J is a linear operator, i.e., $\mathcal{L}_J(a_1g_1 + a_2g_2) = a_1\mathcal{L}_J(g_1) + a_2\mathcal{L}_J(g_2)$ for functions g_1 and g_2 in the domain of \mathcal{L}_J and constants a_1 and a_2 .
- (iv) $\mathcal{L}_u \circ \mathcal{H}_J = 0$, for $u \neq J$.
- (v) $\mathcal{L}_u \circ \mathcal{H}_u = \mathcal{L}_u$.
- (vi) $\mathcal{H}_u \circ \mathcal{H}_J = 0$, for $u \neq J$.
- (vii) $\mathcal{H}_u \circ \mathcal{H}_u = \mathcal{H}_u$.

The statement $\mathcal{L}_u \circ \mathcal{L}_J = 0$ is an abbreviation for $\mathcal{L}_u \circ \mathcal{L}_J(g)(\mathbf{x}) = 0$ for all g and for all \mathbf{x} , and likewise for similar statements. The preceding properties are mostly obvious by inspection of the definitions of \mathcal{L}_J in (A1) and \mathcal{H}_J in (A2)—(A4). Property (i) follows because applying \mathcal{L}_u to a function $g(\mathbf{x}_u)$ that does not depend on $\mathbf{x}_{\setminus u}$ returns the same function $g(\mathbf{x}_u)$ plus lower-order functions of proper subsets of elements of \mathbf{x}_u . Hence, $\mathcal{L}_u \circ \mathcal{L}_u(g)(\mathbf{x}_u) = \mathcal{L}_u(g)(\mathbf{x}_u)$ plus lower order functions, but the sum of these lower-order functions must be identically zero because of the

boundary condition that $\mathcal{L}_u \circ \mathcal{L}_u(g)(\mathbf{x}_u) = \mathcal{L}_u(g)(\mathbf{x}_u) = 0$ when any element of \mathbf{x}_u (say x_j) is at its lower boundary value $z_{0,j}$ over the integration region in (A1). Properties (ii) and (iii) are obvious. Regarding Property (iv), if $u \neq J$, we must have either $u \not\subseteq J$ or $u \subset J$. Property (iv) is obvious for $u \not\subseteq J$, i.e., if u contains at least one index that is not in J . For $u \subset J$, Property (iv) follows by noting that, when applying \mathcal{L}_u to (A3) from left to right, $\mathcal{L}_u \circ (I - \mathcal{L}_\emptyset) \circ \dots \circ (I - \sum_{v \subset J, |v|=|u|-1} \mathcal{L}_v) = \mathcal{L}_u$ (by Property (ii)), so that $\mathcal{L}_u \circ (I - \mathcal{L}_\emptyset) \circ \dots \circ (I - \sum_{v \subset J, |v|=|u|} \mathcal{L}_v) = \mathcal{L}_u \circ (I - \mathcal{L}_u - \sum_{v \subset J, |v|=|u|, v \neq u} \mathcal{L}_v) = \mathcal{L}_u - \mathcal{L}_u - 0 = 0$ (by Properties (i) and (ii)). Property (v) follows similarly. Properties (vi) and (vii) follow immediately from Properties (iv) and (v), respectively.

ALE Decomposition Theorem: A (differentiable) fitted supervised learning model $f(\cdot)$ can be decomposed as $f(\mathbf{x}) = \sum_{J \subseteq D} f_{J,ALE}(\mathbf{x}_J)$, where each ALE component function $f_{J,ALE}$ represents the $|J|$ -order effect of \mathbf{x}_J on $f(\cdot)$. The ALE component functions can be directly constructed via $f_{J,ALE} = \mathcal{H}_J(f)$. Moreover, the ALE component functions have the following orthogonality-like property. For all $J \subseteq D$, we have $\mathcal{H}_J(f_{J,ALE}) = f_{J,ALE}$, and $\mathcal{H}_u(f_{J,ALE}) = 0$ for all $u \subseteq D$ with $u \neq J$. That is, for each $J \subseteq D$, the $|J|$ -order effect of \mathbf{x}_J on $f_{J,ALE}$ is $f_{J,ALE}$ itself, and all other effects on $f_{J,ALE}$ are identically zero. The ALE decomposition is unique in that for any decomposition $f(\mathbf{x}) = \sum_{J \subseteq D} f_J(\mathbf{x}_J)$ with $\{f_J(\mathbf{x}_J): J \subseteq D\}$ having this orthogonality-like property (i.e., with $\mathcal{H}_J(f_J) = f_J$ and $\mathcal{H}_u(f_J) = 0$ for each $J \subseteq D$ and $u \subseteq D$ with $u \neq J$), we must have $f_J(\mathbf{x}_J) = f_{J,ALE}(\mathbf{x}_J)$.

Proof: That $f(\cdot)$ can be decomposed as $f(\mathbf{x}) = \sum_{J \subseteq D} f_{J,ALE}(\mathbf{x}_J)$ follows directly from the definition (A4) of $f_{D,ALE}$ as the residuals. That each $f_{J,ALE}$ can be directly constructed via $f_{J,ALE} = \mathcal{H}_J(f)$ follows from the definition of the operator \mathcal{H}_J . The orthogonality property follows directly from Properties (vi) and (vii). The uniqueness of the ALE decomposition follows trivially from the first parts of the theorem.

Appendix C. Estimation of $f_{J,ALE}(\mathbf{x}_J)$ for Higher-Order Effects

Estimation of $f_{J,ALE}$ for $|J| = 1$ and $|J| = 2$ is described in Section 3. Here we describe estimation of $f_{J,ALE}$ for general $J \subseteq D \equiv \{1, 2, \dots, d\}$. We compute the estimate $\hat{f}_{J,ALE}$ by

computing estimates of the quantities in the composite expression (A3) from right-to-left. Although the notation necessary to formally define $\hat{f}_{J,ALE}$ for general J is tedious, the concept is straightforward: To estimate $\mathcal{L}_J(f)(\mathbf{x}_J)$, we make the following replacements in (A1). We replace $f^J(\mathbf{X}_J, \mathbf{X}_{\setminus J})$ by its corresponding $|J|$ -order finite difference for some appropriate discretization of the \mathbf{X}_J -space; replace $E[f^J(\mathbf{X}_J, \mathbf{X}_{\setminus J})|\mathbf{X}_J = \mathbf{z}_J]$ by its corresponding sample average across all $\mathbf{x}_{i,\setminus J}$ ($i = 1, 2, \dots, n$) for which $\mathbf{x}_{i,J}$ falls into the same discrete cell as \mathbf{z}_J ; and replace the outer integral by the corresponding summation over the same discretization.

More precisely, for any function $g: \mathbb{R}^d \mapsto \mathbb{R}$, we estimate $\mathcal{L}_u(g)(\mathbf{x}_u)$ for $u \subset D$ via

$$\widehat{\mathcal{L}}_u(g)(\mathbf{x}_u) \equiv \sum_{\{\mathbf{k}: 1 \leq k_j \leq K_j(x_j), j \in u\}} \frac{1}{n_u(\mathbf{k})} \sum_{\{i: \mathbf{x}_{i,u} \in N_u(\mathbf{k})\}} \Delta_g^{u,\mathbf{k}}(\mathbf{x}_{i,\setminus u}), \quad (\text{C1})$$

where the notation is as follows. Let $\{N_j(k) = (z_{k-1,j}, z_{k,j}]: k = 1, 2, \dots, K\}$ denote a partition of the sample range of $\{x_{i,j}: i = 1, 2, \dots, n\}$ as in Section 3. We partition the $|u|$ -dimensional range of \mathbf{x}_u into a grid of $K^{|u|}$ rectangular cells obtained as the cross product of the individual one-dimensional partitions. Let $\mathbf{k} = (k_j: j \in u)$ (with each k_j an integer between 1 and K) denote the $|u|$ -length vector of indices into the grid of rectangular cells, let $N_u(\mathbf{k})$ denote the cell associated with \mathbf{k} , and let $\mathbf{z}_{\mathbf{k},u} = (z_{k_j,j}: j \in u)$ denote the $|u|$ -length vector of \mathbf{x}_u values that represents the upper-right corner of $N_u(\mathbf{k})$. Note that the $|u|$ -dimensional rectangle $N_u(\mathbf{k})$ is the Cartesian product of the intervals $\{(z_{k_j-1,j}, z_{k_j,j}]: j \in u\}$. Let $n_u(\mathbf{k})$ denote the number of training observations that fall into $N_u(\mathbf{k})$, so that the sum of $n_u(\mathbf{k})$ over all $K^{|u|}$ rectangles is $\sum_{\{\mathbf{k}: 1 \leq k_j \leq K, j \in u\}} n_u(\mathbf{k}) = n$. For an element (say x_j) of \mathbf{x}_u , let $k_j(x_j)$ denote the index of the interval into which x_j falls, i.e., $x_j \in (z_{k_j(x_j)-1,j}, z_{k_j(x_j),j}]$. Finally, let $\Delta_g^{u,\mathbf{k}}(\mathbf{x}_{i,\setminus u})$ denote the $|u|$ -order finite difference of $g(\cdot)$ with respect to \mathbf{x}_u at $\mathbf{x} = (\mathbf{z}_{\mathbf{k},u}, \mathbf{x}_{i,\setminus u})$. For example, for $u = 1$ and $\mathbf{k} = k$, $\Delta_g^{u,\mathbf{k}}(\mathbf{x}_{i,\setminus u})$ is the first difference $[g(z_{k,1}, \mathbf{x}_{i,\setminus 1}) - g(z_{k-1,1}, \mathbf{x}_{i,\setminus 1})]$. For $u = \{1,3\}$ and $\mathbf{k} = (k, m)$, $\Delta_g^{u,\mathbf{k}}(\mathbf{x}_{i,\setminus u})$ is the difference of the difference $[g(z_{k,1}, z_{m,3}, \mathbf{x}_{i,\setminus \{1,3\}}) - g(z_{k-1,1}, z_{m,3}, \mathbf{x}_{i,\setminus \{1,3\}})] - [g(z_{k,1}, z_{m-1,3}, \mathbf{x}_{i,\setminus \{1,3\}}) - g(z_{k-1,1}, z_{m-1,3}, \mathbf{x}_{i,\setminus \{1,3\}})]$. For general u , $\Delta_g^{u,\mathbf{k}}(\mathbf{x}_{i,\setminus u})$ is the difference of the difference of the difference . . . ($|u|$ times).

The estimate $\hat{f}_{J,ALE}$ is obtained by substituting the estimate (C1) for each term of the form $\mathcal{L}_u(g)(\mathbf{x}_u)$ in (A3). Eqs. (12) and (16) in Section 3 are special cases of $\hat{f}_{J,ALE}$ for $|J| = 1$ and $|J| = 2$.

Appendix D. Some Implementation Details

Vectorization in R. If coding in R, it is important to note that computation of $\hat{f}_{J,ALE}(\mathbf{x}_j)$ is completely vectorizable. For example, to produce the $2^{|J|} \times n$ evaluations of $f(\mathbf{x})$ in (C1) (or in (12) or (16) for ALE main and second-order effects), we can construct a predictor variable array with $2^{|J|} \times n$ rows and d columns and then call the `predict` command (which is available for most supervised learning models in R) a single time. This is typically orders of magnitude faster than using a `for` loop to call the `predict` command $2^{|J|} \times n$ times. Similarly, the averaging and summation operations in (C1), (12), or (16) can be vectorized without the need for a `for` loop. Our R package `ALEPlot` uses this vectorization.

Dealing with empty cells in second-order interaction effect ALE plots. For a second-order interaction effect ALE plot with $J = \{j, l\}$, we discretize the (x_j, x_l) -space into the K^2 rectangular cells by taking the cross product of the individual quantile-based discretizations of x_j and x_l . If (x_j, x_l) are correlated, this will often result in some cells that contain few or no observations. In this case, it may be useful to add scatter plot bullets to the second-order interaction effect ALE plots to indicate the bivariate training sample values $\{(x_{i,j}, x_{i,l}): i = 1, 2, \dots, n\}$. This would help to identify empty cells (i.e., cells with $n_{\{j,l\}}(k, m) = 0$) and, more generally, to identify regions of the (x_j, x_l) -space in which $f_{J,ALE}(\mathbf{x}_j)$ may not be reliable due to lack of data in that region. This is not necessary for main effect ALE plots ($J = j$), because our quantile-based discretization always results in the same number n/K of observations in each region. In the ALE interaction plot of Figure 9, rather than adding scatter plot bullets that represent the training data, we plotted black rectangles to indicate empty cells.

When calculating $\hat{f}_{\{j,l\},ALE}(x_j, x_l)$ via (13), the outer two summations are over a rectangular array of cells. For an empty cell corresponding to $\mathbf{k} = (k, m)$ in this summation, we do not have available the average local effect

$$\frac{1}{n_{\{j,l\}}(k,m)} \sum_{\{i: \mathbf{x}_{i,\{j,l\}} \in N_{\{j,l\}}(k,m)\}} \Delta_f^{\{j,l\},k,m}(\mathbf{x}_{i,\{j,l\}}), \quad (\text{D1})$$

because $n_{\{j,l\}}(k, m) = 0$. In order to allow the outer two summations in (13) to be calculated in this case, we replace the average local effect for an empty cell by the corresponding value for the nearest nonempty cell. This was done for the second-order ALE effect plot in Figure 9 for the income data example, for which there were a number of empty cells indicated by black rectangles. An alternative circumvention is to plot the unaccumulated local effects (D1), instead of the accumulated local effects (16). The discrete differences in (D1) should be divided by the discretized (x_j, x_l) increments in order to have units of second derivative and to account for the fact that the discretization is based on the quantiles, as opposed to a uniform grid. One could then visually assess interactions by inspecting such a plot and looking for any values that differ significantly from zero. However, we do not recommend this approach. For discontinuous supervised learning models such as trees, the discontinuities are amplified by the differencing in (D1), and the resulting plot may be difficult to visualize. The outer summation in (16) tends to smooth discontinuities and other noise and result in more interpretable plots, even with empty cell values replaced by values from their nearest nonempty cell.

The problem of empty cells when constructing a second-order ALE plot is related to, but distinctly different from, the extrapolation problem illustrated in Figure 1(a), which served as motivation for ALE plots. In the context of Figure 1(a), the problem with having a region of empty cells in the (x_j, x_l) -space is that this requires extrapolation when constructing *main effect* PD plots for x_j and x_l . The empty cells present no problem when constructing ALE main effect plots, by design.

Computational tricks for trees. For a tree-based $f(\mathbf{x})$, the weighted tree traversal method (Friedman, 2001) is a clever trick to reduce the computational expense of PD plots. It is doubtful

that this strategy can be adapted for ALE plots. However, considering that the computational expense for direct calculation of ALE plots is already orders of magnitude smaller than for PD plots, further reduction is less important.